Research Square

Preprints are preliminary reports that have not undergone peer review.
They should not be considered conclusive, used to inform clinical practice,
or referenced by the media as validated information.

Projected expansion of Aedes albopictus habitat suitability in Austria under a changing climate

Raphael Spiekermann

Raphael.Spiekermann@geosphere.at

GeoSphere Austria

Johanna Wittholm

GeoSphere Austria

Barbara Seebacher

Austrian Agency for Health and Food Safety

Stefan Kienberger

GeoSphere Austria

Karin Bakran-Lebl

Austrian Agency for Health and Food Safety

Research Article

Keywords: Aedes albopictus, Asian tiger mosquito, invasive species, habitat suitability, climate change, citizen science, expert-based modelling

Posted Date: November 25th, 2026

DOI: https://doi.org/10.21203/rs.3.rs-11431804/v1

License: This work is licensed under a Creative Commons Attribution 4.0 International License.
Read Full License

Additional Declarations: No competing interests reported.

Projected expansion of *Aedes albopictus* habitat suitability in Austria under a changing climate

Raphael Spiekermann[1]*, Johanna Wittholm[1], Barbara Seebacher[2], Stefan Kienberger[1], Karin Bakran-Lebl[2]
[1] GeoSphere Austria, Vienna, Austria
[2] Austrian Agency for Health and Food Safety (AGES), Vienna, Austria
* Corresponding author: *Raphael.Spiekermann@geosphere.at*

Abstract

Background

The Asian tiger mosquito, *Aedes albopictus*, is an invasive vector of dengue, chikungunya and Zika viruses whose European range is expanding through human-mediated dispersal and increasingly favourable climatic conditions. In Austria, the species was first detected in 2012 and has since been reported from all federal states, with established populations in several urban centres such as Vienna and Graz. Because colonisation remains incomplete and occurrence records are spatially biased, current observations may not represent the full range of environments in which the species could establish. We therefore developed a transparent, ecologically and climatologically informed habitat suitability model for data-limited early-colonisation conditions.

Methods

The national-scale model integrates three hierarchically weighted domains: summer climatic suitability, overwintering potential and environmental habitat suitability. Historical climate conditions were represented using SPARTACUS data for 1991–2020. Future projections comprised 2036–2065 under representative concentration pathway (RCP) 8.5 and 2071–2100 under RCP4.5 and RCP8.5, using 16 ensemble members from Austria's regional climate scenarios (ÖKS15). Environmental indicators were derived from Copernicus land-cover products. Habitat suitability classes were derived from ranked index values at verified citizen-science presence locations and applied consistently across scenarios. Climate-

model uncertainty was quantified from the ensemble spread, population exposure was estimated using current and SSP population projection data, and Monte Carlo simulations evaluated sensitivity to expert-derived weights.

Results

Current suitability is concentrated in low-elevation urban and peri-urban areas with relatively mild winters. Across all future scenarios, suitable conditions expand through eastern lowlands and major valley systems. The proportion of Austria classified as Medium to Very high suitability increases from 1.6% during 1991–2020 to 4.8% under late-century RCP4.5 and 6.1% under late-century RCP8.5. Under the latter scenario, 55.7% of the projected population occupies cells classified as High or Very high suitability, compared with 34.1% under reference conditions. Climate uncertainty is greatest in transition zones, particularly parts of the Alpine foreland, whereas several urban hotspots show increasing agreement among ensemble members by late century. The broad spatial pattern was robust to substantially broadened weighting assumptions: under the strongest perturbation setting, the modal class differed from the reference over 0.65% of the modelled area using recalculated thresholds and 2.07% using fixed thresholds.

Conclusions

The framework provides a nationally consistent basis for surveillance prioritisation, vector-control planning and climate adaptation. Its outputs represent relative environmental suitability and population exposure rather than occurrence probability or outbreak risk. The approach is particularly suited to early invasion stages, when available occurrence data remain incomplete and influenced by introduction history and reporting effort.

Keywords: *Aedes albopictus*; Asian tiger mosquito; invasive species; habitat suitability; climate change; citizen science; expert-based modelling

1. Introduction

Climate change is increasingly recognised as a major driver of emerging and expanding vector-borne disease risks in temperate regions (Bouzid et al., 2014; Thomson and Stanberry, 2022). Rising temperatures, milder winters and changing precipitation regimes affect the survival, reproduction, seasonal activity and geographic distribution of arthropod vectors, including mosquitoes (Mordecai et al., 2019; Rocklöv and Dubrow, 2020). These changes can alter both the spatial extent of vector populations and the seasonal window during which pathogens can be transmitted. In northern and western Europe, where Aedes-borne infections have historically been predominantly travel-associated and locally acquired cases were rarely reported, climate warming, urbanisation, land-use change and the increasing movement of people and goods are facilitating vector establishment and raising concern about local arbovirus transmission (ECDC, 2025b; Kraemer et al., 2019).

The Asian tiger mosquito, *Aedes albopictus* (Skuse, 1895), is a particularly important example. Native to parts of Asia, the species has spread globally over recent decades, largely through human-mediated transport, including trade in used tyres and ornamental plants, as well as passive dispersal associated with road traffic and other mobility networks (Swan et al., 2022). It is now established across much of southern and central Europe and continues to expand northward and eastward (ECDC and EFSA, 2025). The species is of public-health relevance because it is a competent vector of several arboviruses, including dengue, chikungunya and Zika viruses (Medlock et al., 2012). While pathogen transmission depends on multiple factors beyond vector presence, including viraemic travellers, vector density, temperature-dependent pathogen development and human exposure, the establishment of *Ae.*

albopictus is a necessary precondition for autochthonous transmission in regions where other competent vectors are absent or rare.

Recent European outbreaks illustrate the growing public-health relevance of this expansion. Autochthonous dengue transmission has repeatedly been reported in Europe, including in France, Italy and Spain. Particularly notable is the increased activity in recent years, peaking in 2024 with 83 cases in France and 213 in Italy (Arulmukavarathan et al., 2024; Santilli et al, 2025; ECDC, 2025a). Chikungunya transmission has also re-emerged in European settings where *Ae. albopictus* is established, with recent reports from France and Italy (Fournier et al., 2025). Such events do not imply uniform risk across Europe, but they demonstrate that once ecological and epidemiological conditions align, local transmission of formerly exotic arboviruses can occur. In this context, identifying where *Ae. albopictus* can establish and persist is a central component of preparedness planning.

In Austria, *Ae. albopictus* was first detected in 2012 (Seidel et al., 2012). Since then, observations have been reported from all federal states, although the status of the species varies spatially from occasional detections to established local populations. Recent ovitrap monitoring and citizen-science records indicate that established populations occur in major urban centres, including Vienna, Graz and Linz (Bakran-Lebl et al., 2021; Bakran-Lebl and Reichl, 2023; Reichl et al., 2024; Situmorang et al., 2025). Lyberger et al. (2025) suggested that the observed expansion may be filling pre-existing thermally suitable habitats driven primarily by anthropogenic factors such as trade and travel. However, warmer winter temperatures facilitate successful colonisation, particularly the +2.3°C warming of winter months (1991–2020 vs. 1850–1900) experienced in the Austrian lowlands (Formayer et al., 2025). Austria therefore represents a region in which *Ae. albopictus* is no longer merely an occasional introduction, but where colonisation remains incomplete and spatially heterogeneous. This situation creates an urgent

need for spatially explicit assessments of current and future habitat suitability that can support surveillance and control while the invasion process is still developing.

Several studies have modelled the potential distribution or climatic suitability of *Ae. albopictus* in Europe (Caminade et al., 2012; Fischer et al., 2011, 2014; Kraemer et al., 2019; Oliveira et al., 2021). These studies have been important for identifying broad-scale climatic constraints and for demonstrating that large areas of Europe may become more suitable under climate change. Multi-model comparisons have shown widespread and increasing suitability for *Ae. albopictus* across European urban areas, with future climatic conditions expected to increase the number of suitable cities (Oliveira et al., 2021). Mechanistic and correlative modelling approaches have likewise indicated that warming may expand suitable regions northward and into areas that were previously limited by winter temperatures or insufficient summer heat (Caminade et al., 2012; Fischer et al., 2011, 2014). More recent work has emphasised that *Ae. albopictus* may rapidly occupy its available climatic niche where introduction pressure and local conditions permit establishment (Radici et al., 2025).

However, continental and macro-regional models necessarily rely on spatial generalisation. They often use coarser climate data, simplified land-surface representations or broad-scale environmental predictors. Such approaches are valuable for continental risk mapping, but they may average out local heterogeneities that are highly relevant for surveillance and control. This limitation is particularly important in Austria, where steep topographic gradients, alpine valleys, lowland basins and urban heat islands generate strong spatial variation in temperature, precipitation and microclimatic conditions over short distances. For local public-health authorities, a continental model may indicate regional suitability but provide insufficient guidance for prioritising monitoring sites or interpreting local establishment risk.

Moreover, *Ae. albopictus* establishment depends not only on climate. Urban and peri-urban environments can increase the availability of artificial larval habitats and alter local microclimates, while residential vegetation and shaded habitats can support adult abundance and persistence (Li et al., 2014; Evans et al., 2019). Sheltered urban infrastructure, particularly stormwater catch basins, may also buffer winter temperatures and improve the overwintering conditions experienced by diapausing eggs (Ravasi et al., 2018, 2022). Therefore, a nationally tailored model should integrate both climatic and land-cover information at a resolution relevant to decision-making.

A further challenge is the early-colonisation status of *Ae. albopictus* in Austria (see Figure 1 and Figure 2). Because the species has not yet occupied all potentially suitable areas, existing occurrence data are unlikely to capture the full range of climatic and environmental gradients across the country. Presence-only data may therefore reflect introduction pathways, reporting effort and current surveillance intensity as much as ecological suitability. Purely data-driven species distribution models risk learning the current sampling pattern rather than the full potential niche, particularly when absence data are unavailable or unreliable. Similarly, dynamic population models require well-characterised demographic parameters, introduction processes and surveillance data that may not yet be available for Austria.

To address these limitations, we developed a national-scale habitat suitability model for *Ae. albopictus* based on high-resolution, nationally available climate and land-cover datasets. The model uses an expert-informed hierarchical index framework that integrates ecological knowledge about overwintering constraints, summer climatic suitability and environmental habitat characteristics. The approach is specifically designed to be transparent, interpretable and applicable in data-sparse settings. It does not attempt to infer the species' niche exclusively from incomplete occurrence data; instead, it combines established ecological thresholds and habitat-relevant indicators into spatially explicit suitability estimates that can be evaluated against available presence data and updated as monitoring improves.

Specifically, this study aims to: (1) delineate the current spatial distribution of climatically and environmentally suitable areas for *Ae. albopictus* in Austria; (2) project potential future changes in habitat suitability under representative concentration pathway (RCP) 4.5 and RCP8.5 climate scenarios for mid-century and late-century periods; (3) classify habitat suitability using observed presence locations and assess how projected suitability classes change over time; (4) quantify and visualise climatic uncertainty using ensemble climate projections; (5) estimate population exposure to current and future habitat suitability classes using Statistics Austria and the so-called Shared Socioeconomic Pathways (SSPs) population data; and (6) evaluate the sensitivity of model outputs to expert-derived weighting assumptions.

2. Methods

Study area

The study area comprises the entire territory of Austria, covering approximately 83,900 km² (Figure 2). Austria is characterised by strong topographic and climatic gradients, ranging from lowland regions in the east and southeast to high alpine terrain in the west and central Austria. Elevation, continentality and alpine topography generate pronounced spatial variation in temperature and precipitation. These gradients are particularly relevant for *Ae. albopictus*, whose establishment is constrained by winter survival, summer developmental conditions and the availability of suitable anthropogenic and vegetated microhabitats (Medlock et al., 2006, 2012; Li et al., 2014; Evans et al., 2019). Urban areas in Austria are concentrated mainly in lowland and valley settings, including the major cities of Vienna, Graz, Linz, Salzburg, and Innsbruck. These areas combine relatively mild microclimates, high human population density, potential introduction pathways and artificial breeding habitats. At the same time, the alpine landscape contains extensive regions where low winter temperatures and short warm seasons may

currently limit establishment. The strong environmental heterogeneity of Austria provides a useful test case for a national-scale model that integrates high-resolution climate and land-cover information.

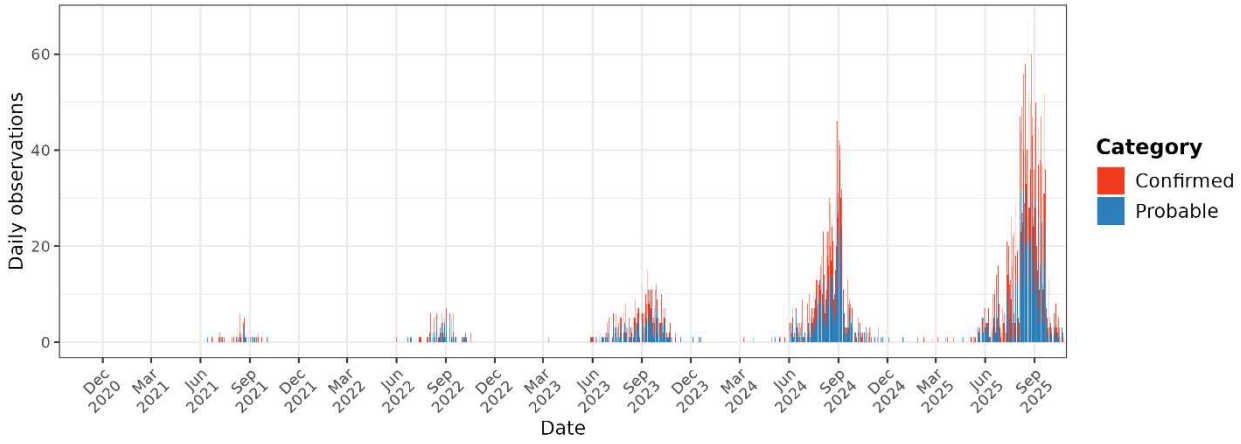


Figure 1. Daily Mosquito Alert observations from 2020 to 2025 (n = 4,561 records).

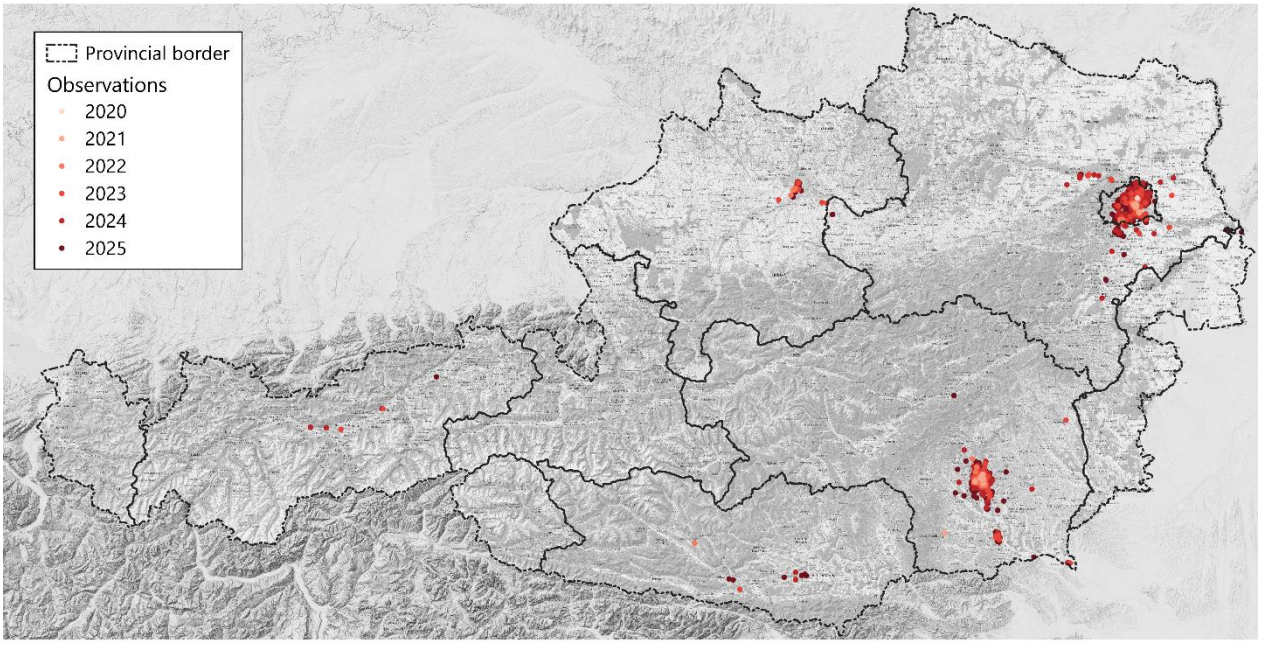


Figure 2. Map of Austria showing verified Ae. albopictus Mosquito Alert observations from 2020 to 2025.

Data and model

2.1.1. Modelling framework

We developed a hierarchical habitat suitability index for *Ae. albopictus* at a spatial cell resolution of 1 km, corresponding to the resolution of the national climate inputs. The model integrates indicators from three thematic domains representing complementary ecological constraints and habitat requirements, referred to as: (i) overwintering potential, (ii) summer climatic suitability and (iii) environmental habitat suitability. Indicators were selected from published ecological evidence and expert judgement, transformed so that higher values consistently indicated greater suitability, and aggregated within domains using weighted arithmetic means. The indicator and domain weights were selected during an expert workshop, informed by a literature review and expert judgement. The resulting domain indices were subsequently combined into the final habitat suitability index (Figure 3). Because weighted linear aggregation is partially compensatory, unfavourable conditions represented by one indicator can be offset by favourable values of other indicators in proportion to their assigned weights; indicators representing adverse conditions were inverted where necessary prior to aggregation. Before aggregation, indicators requiring transformation were rescaled to a common 0–1 range using Min–Max standardisation:

$$x^*_{c,j} = \frac{(x_{c,j} - x_{j,min})}{(x_{j,max} - x_{j,min})}$$

$x_{c,j}$ is the original value of indicator j in grid cell c, and $x_{j,min}$ and $x_{j,max}$ the corresponding scaling bounds of the indicator. Indicators negatively related to habitat suitability were inverted as:

$$x^*_{c,j,inv} = 1 - x^*_{c,j}$$

Within each domain d, the standardised indicators were aggregated by weighted arithmetic mean:

$$D_{c,d} = \sum_{j=1}^{k_d} w_{d,j}\, x^{*}_{c,d,j}$$

$$with \quad \sum_{j=1}^{k_d} w_{d,j} = 1$$

where $D_{c,d}$ is the suitability score for domain d in grid cell c, k_d is the number of indicators in that domain, and $w_{d,j}$ is the weight assigned to indicator j.

The model was implemented for the historical reference period 1991–2020 and for three future climate conditions: 2036–2065 under RCP8.5 (since RCP4.5 is very similar for this period), and 2071–2100 under RCP4.5 and RCP8.5. RCPs are climate-forcing scenarios defined by the IPCC (2014), which consist of four different 21st century pathways of greenhouse gas emissions, atmospheric concentrations, air pollutants and land-use change. In this study, we have selected two of these scenarios: RCP4.5 represents an intermediate stabilisation pathway in which radiative forcing stabilises at approximately 4.5 W m^{-2} after 2100, whereas RCP8.5 represents a high-forcing pathway reaching more than 8.5 W m^{-2} by 2100. Climate-dependent indicators were recalculated separately for each climate-model ensemble member. Present day land-cover indicators were used for all periods, so projected changes isolate the effect of climate and do not include future urbanisation, vegetation change or land-management trajectories.

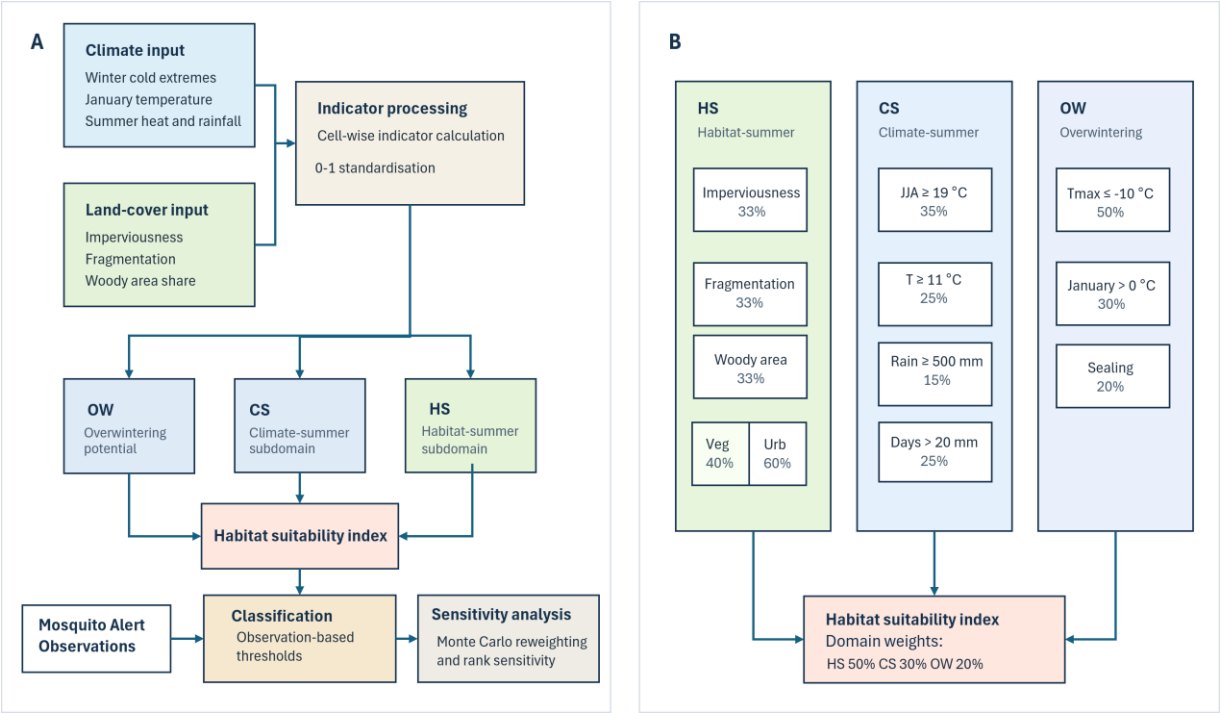


Figure 3. Conceptual workflow and weighting structure of the hierarchical habitat suitability model for Ae. albopictus in Austria. (A) Overview of climate and land-cover inputs, cell-wise indicator calculation, 0–1 standardisation, aggregation into the overwintering potential (OW), summer climatic suitability (CS) and environmental habitat suitability (HS) domains, observation-based classification and weight-sensitivity analysis. (B) Expert-derived indicator and domain weights used in the final model. Domain weights were 50% for HS, 30% for CS and 20% for OW.

2.1.2. Climate data and uncertainty

Historical climate indicators were derived from the SPARTACUS version 2 daily temperature and precipitation grids, which are based on spatial kriging of Austrian station observations (Hiebl and Frei, 2016, 2018). SPARTACUS represented the 1991–2020 reference period and was selected because it was developed for national hydroclimatic applications and captures Austria's pronounced alpine–lowland climatic gradients more directly than coarser continental products. Indicator values were calculated for each raster cell over the complete 30-year period.

Future climate conditions were represented using the ÖKS15 Austrian regional climate scenarios (Chimani et al., 2016), which are widely used in national climate-impact assessments (e.g. Unterberger et

al., 2018; Thaler et al., 2021). Three scenario-period combinations were assessed: 2036–2065 under RCP8.5 and 2071–2100 under RCP4.5 and RCP8.5. For each combination, all climate-dependent indicators were calculated separately for 16 climate ensemble members. The 16 ÖKS15 ensemble members represent different combinations of global and regional climate-model simulations downscaled for Austria, and were used here to propagate climate-model spread through the habitat-suitability workflow rather than relying on a single climate projection. Every member was processed through the complete modelling workflow, including indicator standardisation, domain-level aggregation and calculation of the final habitat suitability index. The ensemble-mean of the 16 member-specific HSI maps was used to represent the central projection for each scenario.

Climate-model uncertainty was quantified as the cell-wise standard deviation among the 16 HSI realisations. Mean suitability and ensemble spread were visualised jointly using 4 × 4 bivariate maps following Schlögl et al. (2025). Ensemble-mean suitability was divided into four classes using observation-derived HSI thresholds, while uncertainty was classified using quartiles of the pooled grid-cell standard deviations from the three future scenarios. Applying common uncertainty breaks ensured direct comparability among scenarios. Cells combining high mean suitability with low ensemble spread represent comparatively consistent projected hotspots, whereas high-suitability cells with greater spread indicate locations where projections depend more strongly on the climate realisation.

The ensemble standard deviation represents uncertainty among the selected ÖKS15 projections only. It does not account for uncertainty associated with emissions pathways beyond those assessed, future land-cover change, ecological thresholds, introduction pressure, biological adaptation or the structural assumptions of the habitat suitability model. The climate indicators included in the model are specified in sections 2.2.4 to 2.2.6.

2.1.3. Land-cover data

Environmental habitat indicators were derived from Copernicus Land Monitoring Service products. The principal inputs were the 2018 Imperviousness Density layer and thematic classes from the 2021 CLC+ Backbone raster, both at 10 m native resolution (Table 1). The source layers were projected where required, aligned to the national reference grid prior to aggregation to 1 km. These data were used to represent settlement intensity, sealed surfaces, woody vegetation and the structural intermixing of built and open land relevant to breeding-site availability and local microclimatic conditions.

Specifically, three indicators characterised environmental structure within each 1 km^2 cell. Imperviousness density (V1) was the proportion of sealed surface on a continuous 0-100% scale and served as a proxy for built-up and peri-urban environments with high densities of artificial containers and human hosts. The combined fragmentation index (V2) was calculated from normalised settlement density (SDI_norm) and settlement efficiency ($FI = SDI_{norm} \times SEI$) and represented the intermixing of built, open and vegetated areas. The third indicator (V3) was the proportion of woody vegetation, including trees and shrubs, and represented shading, moisture retention and microclimatic buffering. These mechanisms are relevant to adult resting habitat and the persistence of small aquatic breeding sites, although their effects may vary among local habitat types.

The three environmental indicators were standardised to a common 0–1 scale and combined with equal weights to form a landscape habitat index. A separate urbanisation indicator was derived from sealed residential or settlement classes and aggregated to 1 km. The environmental habitat suitability domain combined urbanisation and the landscape habitat index with weights of 0.60 and 0.40, respectively. The higher urbanisation weight reflects the strong association of *Ae. albopictus* with residential and peri-urban habitats, while the landscape component retains information on vegetation and spatial habitat structure.

Land-cover indicators were treated as static in all future simulations. Projected differences therefore represent climate-driven changes conditional on the 2018/2021 land-cover configuration. This avoids introducing an additional speculative land-use scenario but may underestimate suitability where future settlement growth, water-storage practices or vegetation change alter anthropogenic habitats.

Table 1 Summary of datasets and derived indicators used in the habitat suitability and exposure analyses.

Data type	Dataset	Spatial resolution	Period / scenario	Derived indicators	Used in model domain
Historical temperature	SPARTACUS daily temperature grids	1 km	1991–2020	Average extreme colddays with Tmax ≤ −10 °C per year; Fraction of years withmean January temperature > 0 °C; Fraction of years with mean JJA temperature ≥ 19 °C; Fraction of years with annual mean temperature ≥ 11 °C	Overwintering potential; summer climatic suitability
Historical precipitation	SPARTACUS daily precipitation grids	1 km	1991–2020	Fraction of years with annual precipitation > 500 mm; Average number of precipitation events > 20 mm day^{-1} during March–September per year	Summer climatic suitability
Future temperature projections	ÖKS15 climate scenarios	1 km	2036–2065 under RCP8.5; 2071–2100 under RCP4.5 and RCP8.5	Same temperature-based indicators as for SPARTACUS, recalculated for each ensemble member	Overwintering potential; summer climatic suitability
Future precipitation projections	ÖKS15 climate scenarios	1 km	2036–2065 under RCP8.5; 2071–2100 under RCP4.5 and RCP8.5	Same precipitation-based indicators as for SPARTACUS, recalculated for each ensemble member	Summer climatic suitability
Climate ensemble members aggregations	ÖKS15 ensemble	1 km	16 ensemble members per future scenario	Ensemble mean and standard deviation of habitat suitability	Climate uncertainty assessment
Imperviousness	Copernicus Imperviousness Density Layer	10 m, aggregated to 1 km	2018	Imperviousness density / sealing degree (fraction)	Environmental habitat suitability; overwintering potential
Land-cover classes	Copernicus CLC+ Backbone raster	10 m, aggregated to 1 km	2021	Sealed surfaces, woody vegetation, grassland / non-sealed vegetation classes (fraction)	Environmental habitat suitability
Landscape structure	Derived from Copernicus land-cover products	10 m, aggregated to 1 km	2018 / 2021	Fragmentation degree / combined fragmentation index	Environmental habitat suitability
Population baseline	Statistik Austria population data	100 m, aggregated to 1 km	2020	Population exposed by habitat suitability class	Exposure analysis

Data type	Dataset	Spatial resolution	Period / scenario	Derived indicators	Used in model domain
Future population projections	PopAUT SSP population grids	1 km	SSP2 and SSP5; 2050 and 2085	Future population exposed by habitat suitability class	Future exposure analysis
Observation data	Mosquito Alert citizen-science observations	Point data	2020–2025	Index values at positive observation locations	Classification

2.1.4. Overwintering potential

The overwintering potential domain represents the capacity of diapausing *Ae. albopictus* eggs to survive winter conditions and contribute to population persistence in the following season. It comprised three indicators: severe cold days, mean January temperature and urbanisation (Figure 3). Winter survival is a major range-limiting process in temperate regions, but conditions in sheltered urban microhabitats can differ from gridded meteorological estimates (Ravasi et al., 2018, 2022).

The severe-cold indicator was defined as the mean annual number of days on which daily maximum temperature was ≤ −10 °C during the respective climate period. Experimental studies indicate that prolonged exposure near −10 °C approaches the lower survival limit of post-diapause eggs from European *Ae. albopictus* strains (Thomas et al., 2012). Because more severe-cold days reduce suitability, the standardised indicator was inverted. The second indicator was the proportion of years with mean January temperature > 0 °C. The 0 °C January isotherm has been used as a conservative approximation of the northern overwintering limit (Nawrocki and Hawley, 1987; Medlock et al., 2006). The third indicator was imperviousness density, included as a proxy for urban thermal buffering and sheltered anthropogenic microhabitats. Measurements in Swiss cities showed that stormwater catch basins provided warmer and more thermally stable winter microhabitats than nearby outdoor conditions, potentially reducing exposure of diapausing *Ae. albopictus* eggs to lethal cold events (Ravasi et al., 2018, 2022).

As with the other domains, the indicators were standardised to a common 0–1 scale where required. Future severe-cold values were transformed using the SPARTACUS reference-period minimum and maximum to retain temporal comparability. The domain index was calculated using weights of 0.50 for severe cold, 0.30 for January temperature > 0 °C and 0.20 for urbanization (Figure 3). This assigns greatest influence to potentially lethal cold exposure while allowing broader winter conditions and urban microclimatic buffering to modify suitability.

2.1.5. Summer climatic suitability

The summer climatic suitability domain represents thermal and moisture conditions relevant to larval development, adult activity and reproduction. It contains four indicators: the proportion of years with mean June - August temperature ≥ 19 °C, the proportion of years with annual mean temperature ≥ 11 °C, the proportion of years with annual precipitation > 500 mm, and the mean annual number of days with precipitation > 20 mm during March - September. The temperature and annual-precipitation thresholds were selected from previous European assessments of *Ae. albopictus* climatic suitability (Caminade et al., 2012; Fischer et al., 2011, 2014; Medlock et al., 2006).

Annual precipitation >500 mm was used as a broad indicator of adequate water availability. Heavy rainfall can have contrasting effects on container-breeding mosquitoes: it can replenish aquatic habitats but can also flush immature stages or remove nutrients from small and exposed containers (Benedum et al., 2018; Koenraadt and Harrington, 2008). In the present index, frequent March-September events >20 mm day^{-1} were treated as a potential disturbance and the standardised indicator was therefore inverted.

The four indicators were standardised where required and combined using weights of 0.35 for mean summer temperature ≥19 °C, 0.25 for annual mean temperature ≥ 11 °C, 0.15 for annual precipitation >500 mm and 0.25 for heavy-rainfall frequency. In line with the treatment of other indicators, the heavy-rainfall indicator was standardised using a minimum of zero and the maximum across the complete

future ensemble to maintain a common scale among scenarios. The weighting gives greatest importance to sustained summer warmth while retaining broader thermal, moisture and disturbance constraints.

2.1.6. Environmental habitat suitability

The environmental habitat suitability domain represents land-cover and settlement characteristics affecting breeding-site availability, adult resting habitat and local microclimate (Figure 3). The ecological interpretation of the indicators is described in Section 2.2.3; Imperviousness density, the combined fragmentation index and woody vegetation were each assigned one third of the weight in the landscape habitat index. Imperviousness represents built-up environments and artificial-container density; fragmentation represents mixed settlement–vegetation mosaics; and woody vegetation represents shading and moisture retention. These predictors describe environmental opportunity rather than human-mediated introduction pressure, which was not included explicitly. The landscape habitat index was combined with the separate urbanisation indicator using weights of 0.40 and 0.60, respectively. The resulting environmental habitat suitability domain thus emphasises settlement-associated habitat while retaining variation in vegetation and landscape structure.

2.1.7. Habitat suitability index and classification

The final habitat suitability index (HSI) was calculated as

$$HSI_c = \sum_{d=1}^{3} W_d \, D_{c,d} \; = 0.5D_{c,HS} \; + \; 0.3D_{c,CS} \; + \; 0.2D_{c,OW}$$

where W_d denotes the domain-level weight, and HS, CS and OW denote environmental habitat suitability, summer climatic suitability and overwintering potential, respectively. The index is a relative, dimensionless score and not an occurrence probability. The selected domain weights reflect the working ecological assumption that settlement-associated habitat strongly structures local establishment opportunity, while summer climate and winter persistence determine climatic feasibility. In the

sensitivity analysis, this final expert weighting is referred to as the reference weighting (see Supplementary Material).

Verified Mosquito Alert records from January 2020 to December 2025 were used for presence-based calibration and plausibility assessment of the HSI. Mosquito Alert is a citizen science project where submissions are assigned taxonomic categories through expert validation (Južnič-Zonta et al., 2022). Both confirmed (2185) and probable (2376) records were included, yielding N = 4561 adult tiger mosquito observations. Because reporting effort is concentrated in populated and accessible locations, and because colonisation by the species remains incomplete, the records were not treated as a representative sample of the national environmental gradient and were not used to fit a correlative occurrence model.

Reference-period HSI values were extracted at all retained presence locations. The 1st, 10th, 25th and 50th percentiles of this distribution defined five relative suitability classes: very low (<p1), low (p1–p10), medium (p10–p25), high (p25–p50) and very high (≥p50). Thus, p1 marks a value below which only 1% of retained observations occurred, whereas at least half of the observations occurred at or above p50 (Figure 4). The thresholds were derived once from the 1991–2020 HSI and applied unchanged to all climate scenarios, enabling direct temporal comparison. The classes express relative similarity to conditions at reported presence locations and are not biological establishment thresholds or calibrated occurrence probabilities.

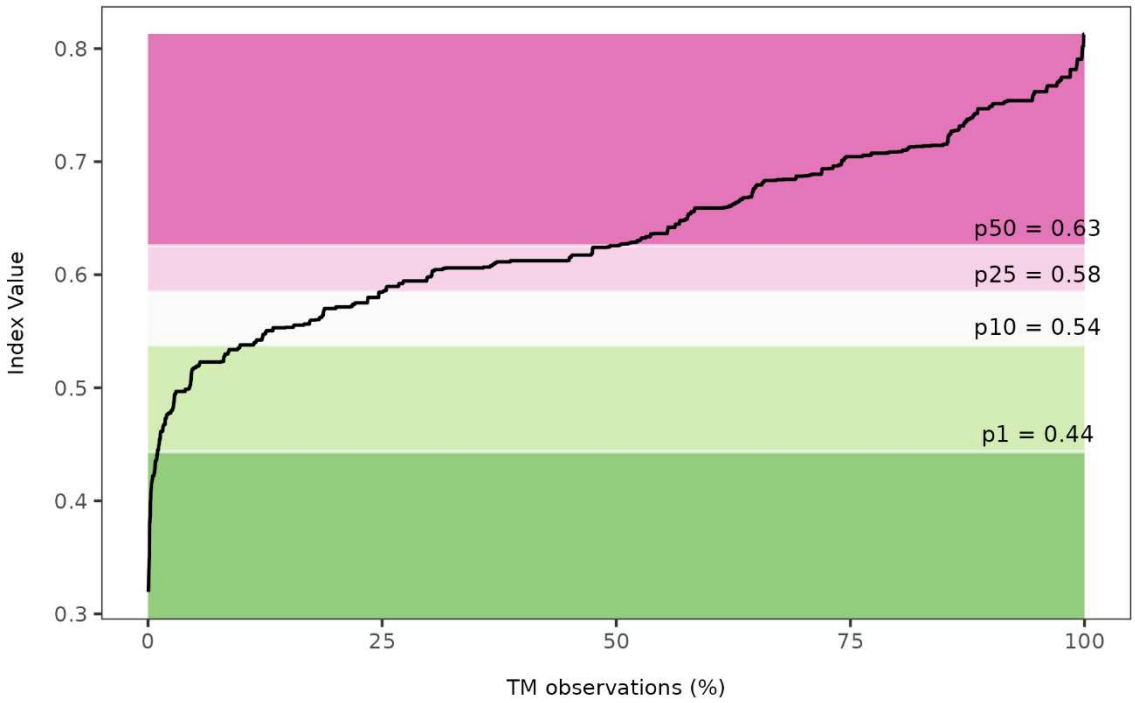


Figure 4. The derivation of class boundaries is based on the quantiles (p1 – p50) of the ranked index values at the presence locations.

Because the classification is derived from the expert-weighted HSI, we evaluated its robustness using a Monte Carlo sensitivity analysis in which domain and indicator weights were repeatedly perturbed and the resulting HSI values and class assignments were recalculated. The full sensitivity analysis is presented in the Supplementary Material and assesses both continuous HSI variation and reference-class agreement under alternative plausible weighting configurations.

2.1.8. Population exposure

To add the societal dimension to the suitability assessment, we quantified the number of residents located in cells assigned to each HSI class estimate potentially affected population numbers today and in the future. This quantity is termed population exposure to suitable habitat; it is not intended to represent mosquito abundance, human-vector contact or epidemiological risk. For the reference period, population counts were obtained from the Statistik Austria 100 m grid for persons with primary

360 residence (Hauptwohnsitz, attribute *hws*; data status 1 January 2022). 100 m cell centroids were used to
361 assign each population cell to one 1 km^2 suitability class, and *hws* counts were summed by class.

362 Future population was obtained from the Pop-AUT subnational Shared Socioeconomic Pathways (SSPs)
363 projections for Austria (Marbler, 2024), available at five-year intervals. SSP2 (“Middle of the Road") was
364 combined with the late-century RCP4.5 suitability scenario and SSP5 (Fossil-fueled Development -
365 "Taking the Highway") with late-century RCP8.5. These pairings follow the commonly used SSP–RCP
366 combinations in the global climate impact literature, although at the regional scale alternative SSP–RCP
367 combinations are also plausible and may be equally valid depending on the socioeconomic and policy
368 assumptions. The 2050 population layer was used for 2036–2065 and the 2085 layer for 2071–2100. For
369 the mid-century RCP8.5 suitability map, SSP2-2050 was used as a pragmatic central demographic
370 projection rather than as a formally paired SSP5–RCP8.5 scenario. Future population rasters were
371 projected to the 1 km habitat grid using population-preserving summation and masked to Austria.

372 For each scenario, population was summed within the five suitability classes. Baseline exposure was
373 calculated from the Statistik Austria centroid overlay, whereas future exposure was calculated by zonal
374 summation of the Pop-AUT raster. Because the baseline and future layers originate from different
375 population products and demographic assumptions, temporal differences reflect both projected
376 demographic change and changing habitat suitability. Results are therefore reported as scenario-specific
377 exposure rather than as change attributable solely to climate.

378 Population exposure for scenario s and suitability class k can be expressed as:

379 $$E_{s,k} = \sum_{c \in C_{s,k}} P_{s,c}$$

380 where $E_{s,k}$ is the exposed population, $P_{s,c}$ is the population assigned to grid cell c, and $C_{s,k}$ is the set
381 of cells classified as suitability class k under scenario s.

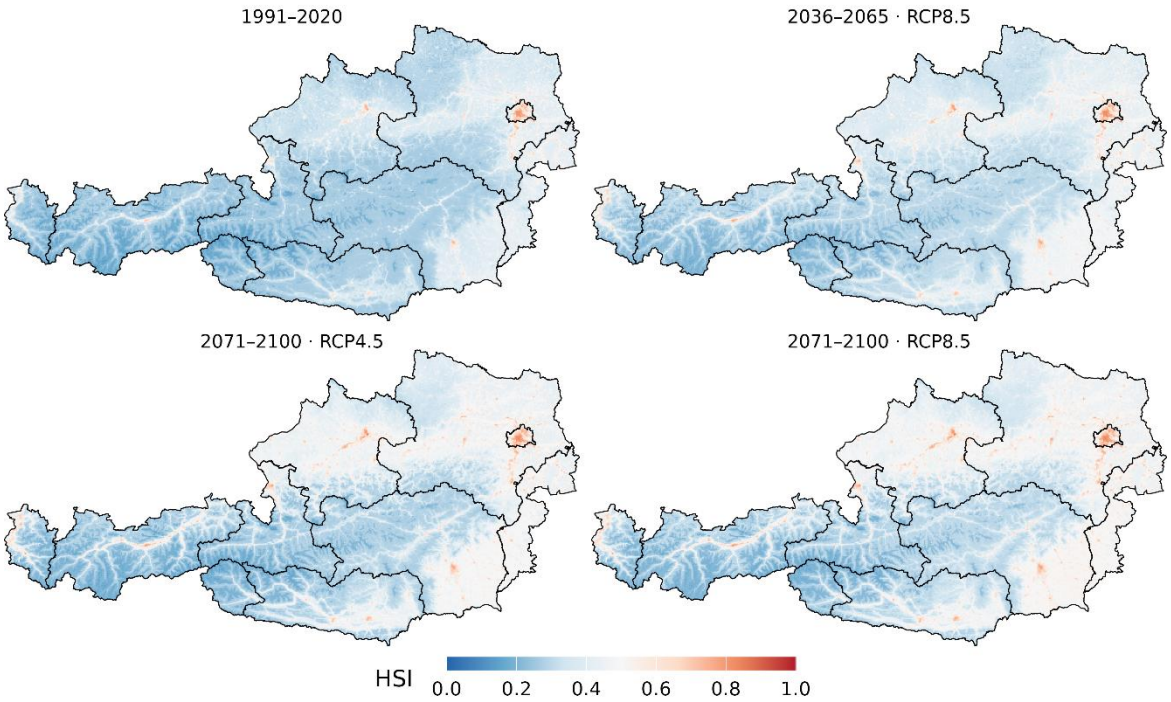
3. Results

Habitat suitability

Under 1991–2020 conditions, the continuous HSI was dominated by low values across much of Austria, while locally elevated values occurred in low-elevation urban areas. The highest values were concentrated in and around Vienna, Graz, Linz and other urban or peri-urban lowlands. Large parts of the alpine west and central mountain regions remained below the observation-derived p1 threshold. The national HSI distribution was strongly concentrated below 0.5, with only a small upper tail crossing the medium, high and very-high class thresholds (Figure 5).

The overwintering potential was greatest in mild lowlands and urban areas, whereas cold alpine regions remained strongly constrained. Summer climatic suitability followed broad lowland and valley temperature gradients, and environmental habitat suitability was concentrated around settlement and peri-urban land-cover mosaics. Areas of high final HSI occurred where these complementary patterns overlapped.

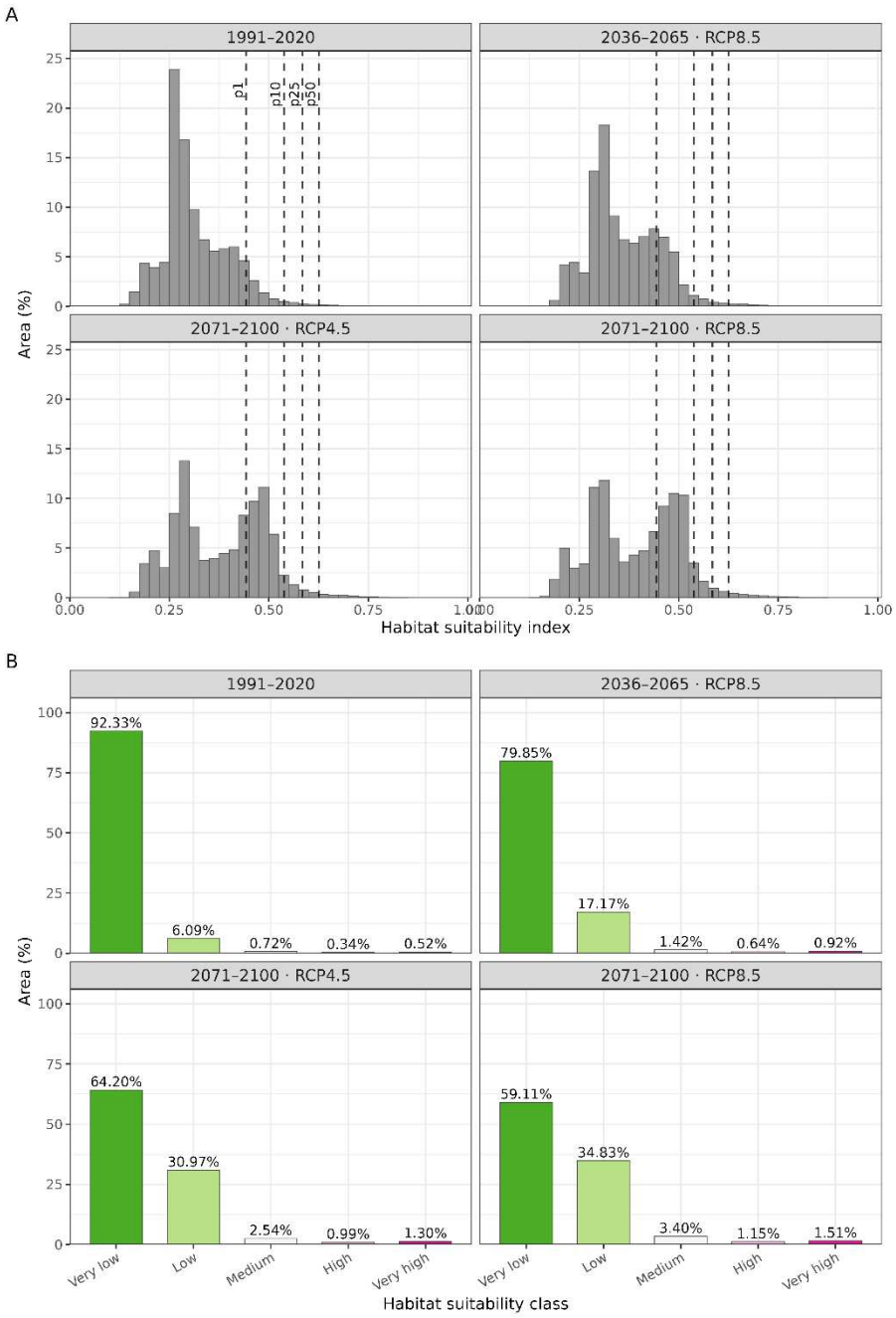
Continuous HSI values increased under all three future scenarios (Figure 5). The distribution shifted towards higher values and a larger share of the national grid crossed the fixed presence-derived thresholds (Figure 6A). The shift was evident by 2036–2065 under RCP8.5 and was stronger by 2071–2100, particularly under RCP8.5. The late-century distributions also broadened, indicating that warming increased suitability in some lowland and valley regions while large alpine areas remained comparatively unsuitable.



404

405 *Figure 5. Habitat suitability index (HSI) for the historical period (1991–2020), the mid-century period from*
406 *2036–2065 under RCP8.5, and the two late-century periods from 2071–2100 under both RCP4.5 and*
407 *RCP8.5.*

408



409

410 *Figure 6. A) Distribution of continuous habitat suitability index values across Austria for the reference*
411 *period (1991–2020) and three future climate scenarios; dashed vertical lines indicate the observation-*
412 *derived classification thresholds (p1, p10, p25 and p50), which were held constant across scenarios. (B)*
413 *Percentage of Austria's modelled area assigned to each of the five habitat suitability classes under the*
414 *corresponding scenarios, with percentage values shown.*

Spatial expansion was concentrated in eastern and southeastern lowlands, urban corridors and major valley systems. Existing urban hotspots remained among the highest-suitability locations, while surrounding areas shifted predominantly from very low to low or medium classes. In alpine regions, increases followed lower valleys, particularly the Danube river valley, and basin margins rather than high-elevation terrain, demonstrating that warming reduced but did not remove topographic constraints.

Applying the fixed observation-derived thresholds translated the continuous shift into a redistribution among suitability classes (Figure 6B and Figure 7). Under reference conditions, Medium, High and Very high suitability together covered approximately 1.6% of Austria (Table 2). The tabulated distribution shows that most of the country remained in the Very low class in every scenario, but the Low and Medium classes expanded progressively under future climate conditions. By 2071–2100, the combined Medium-to-Very-high area increased to approximately 4.8% under RCP4.5 and 6.1% under RCP8.5. Most of this expansion occurred in the medium class, while High and Very high suitability remained spatially restricted to localised urban and peri-urban cores.

The classified maps identify persistent high-suitability cores around established or repeatedly observed urban populations and broader emerging zones of medium suitability. The latter represent potential surveillance frontiers to confirm future establishment, particularly where introduction pressure is unknown. Difference maps can support identifying areas with the greatest expected change due to a warming climate (see Supplementary Figure 1).

Table 2. Modelled area of Austria within each habitat suitability class for the reference period and three future climate scenarios. Values are reported as area in km², with the percentage of the valid modelled territory in parentheses.

Scenario	Very low	Low	Medium	High	Very high

1991–2020	77,450 km² (92.33%)	5,105 km² (6.09%)	606 km² (0.72%)	286 km² (0.34%)	437 km² (0.52%)
2036–2065, RCP8.5	66,982 km² (79.85%)	14,403 km² (17.17%)	1,192 km² (1.42%)	539 km² (0.64%)	768 km² (0.92%)
2071–2100, RCP4.5	53,856 km² (64.20%)	25,981 km² (30.97%)	2,130 km² (2.54%)	827 km² (0.99%)	1,090 km² (1.30%)
2071–2100, RCP8.5	49,580 km² (59.11%)	29,219 km² (34.83%)	2,853 km² (3.40%)	968 km² (1.15%)	1,264 km² (1.51%)

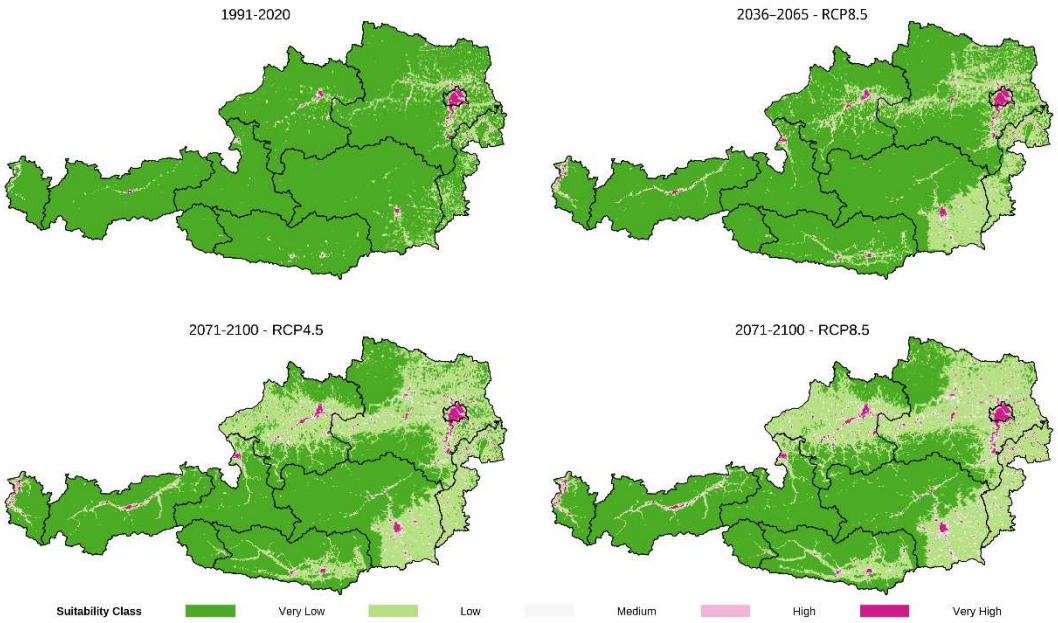


Figure 7. Classified habitat suitability maps for the historical period (1991–2020), the mid-century period from 2036–2065 under RCP8.5, and the two late-century periods from 2071–2100 under both RCP4.5 and RCP8.5

Climate-model uncertainty

The 16-member ensemble consistently projected increased suitability, but the magnitude and local extent of change varied among climate realisations (Figure 8). The bivariate maps combine four classes of ensemble-mean habitat suitability with four classes of climate-model uncertainty. Suitability classes (S1–S4) were defined using three presence-derived thresholds from the reference model—p1 = 0.4434, p10 = 0.5379 and p50 = 0.6256—to produce four classes for visualisation. Uncertainty classes (U1–U4) were based on pooled quartiles of the ensemble standard deviation across all three future scenarios: Q1 = 0.0084, Q2 = 0.0172, Q3 = 0.0282.

The bivariate distributions were dominated by combinations of low suitability and varying levels of climate-model uncertainty (Table 3). In the mid-century RCP8.5 scenario, 79.8% of the modelled area remained in the lowest suitability class (S1), with the largest shares assigned to S1–U1 (25.33%) and S1–U3 (28.85%). By late century, the proportion of low-suitability area associated with the highest uncertainty class increased, with S1–U4 accounting for 22.27% under RCP4.5 and 33.29% under RCP8.5. Spatially, the largest uncertainty hotspots occurred mainly in the Alpine foreland and other climatic transition zones, although these areas generally retained low modelled suitability.

Higher-suitability areas were comparatively limited and were generally associated with lower or moderate ensemble spread. Several urban areas, including Klagenfurt and Villach in Carinthia and the city of Salzburg, were projected to have relatively high suitability but also high climate-model uncertainty under the mid-century RCP8.5 scenario. Under late-century RCP8.5, uncertainty in these cities decreased as the warming signal became more consistent across the ensemble, resulting in stronger agreement on favourable climatic conditions. More broadly, S2–U1 accounted for 19.94% of the modelled area under late-century RCP8.5, indicating a substantial expansion of low-to-moderate suitability under comparatively consistent projections. In contrast, the combination of highest suitability and highest

uncertainty remained extremely rare, with S4–U4 representing no more than 0.05% of the modelled area in any scenario.

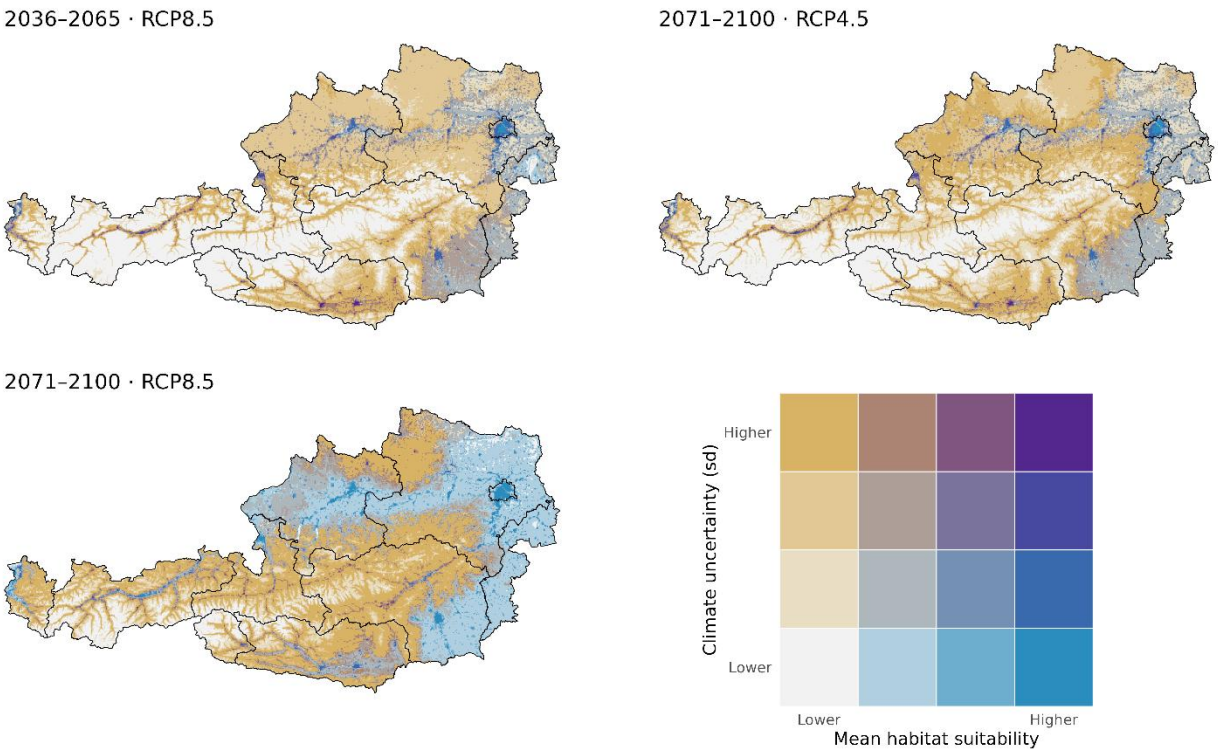


Figure 8. Projected mean Ae. albopictus habitat suitability and climate-model uncertainty for the three future scenarios. Colours combine four classes of ensemble-mean suitability with four quantile-based classes of ensemble standard deviation; the bivariate legend indicates increasing suitability from left to right and increasing uncertainty from bottom to top.

Table 3. Proportion of Austria's valid modelled area assigned to each bivariate habitat suitability–climate uncertainty category under the three future scenarios. Categories combine four classes of ensemble-mean suitability (S1–S4, from lower to higher suitability) with four classes of ensemble standard deviation (U1–U4, from lower to higher climate-model uncertainty); common class breaks were applied across scenarios to ensure comparability.

Bivariate category	2036–2065 · RCP8.5	2071–2100 · RCP4.5	2071–2100 · RCP8.5
S1-U1	25.33%	18.89%	5.61%
S1-U2	14.04%	21.10%	7.29%
S1-U3	28.85%	17.99%	7.13%
S1-U4	11.62%	22.27%	33.29%
S2-U1	0.32%	0.01%	19.94%
S2-U2	7.48%	9.64%	10.45%
S2-U3	7.72%	5.44%	6.14%
S2-U4	1.66%	1.76%	3.86%
S3-U1	0.05%	0.01%	3.36%

S3-U2	1.21%	1.30%	1.10%
S3-U3	0.62%	0.54%	0.21%
S3-U4	0.18%	0.17%	0.10%
S4-U1	0.10%	0.12%	1.26%
S4-U2	0.60%	0.57%	0.23%
S4-U3	0.17%	0.16%	0.02%
S4-U4	0.05%	0.04%	0.01%

Population exposure to habitat suitability classes

Population exposure in the reference period was predominantly concentrated in suitability classes associated with densely populated urban and lowland areas (Figure 9). However, population exposure shifts progressively towards higher suitability classes across the future scenarios. Under reference conditions, 34.1% of the population resided in cells classified as High or Very high suitability, increasing to 39.3% for 2036–2065 under RCP8.5, 46.0% for 2071–2100 under RCP4.5, and 55.7% for 2071–2100 under RCP8.5 (Table 4) assuming SSP2 for future scenarios. The share of the population in the Very high class alone rose from 27.6% historically to 47.3% under late-century RCP8.5, corresponding to an increase from approximately 2.48 million to 5.02 million residents. Conversely, the proportion living in Very low suitability areas declined from 37.4% to 9.2%, indicating a substantial redistribution of population exposure towards more environmentally receptive areas.

Table 4. Population exposed to modelled Ae. albopictus habitat suitability classes under the historical and future scenarios. Values show the estimated number of residents within each suitability class, with the percentage of the scenario-specific total population in parentheses. Population counts are rounded to the nearest person.

Scenario	Total population	Very low, n (%)	Low, n (%)	Medium, n (%)	High, n (%)	Very high, n (%)
1991–2020	8,970,554	3,352,541 (37.37%)	1,762,340 (19.65%)	800,393 (8.92%)	579,936 (6.46%)	2,475,344 (27.59%)
2036–2065, RCP8.5–SSP5	9,238,702	2,395,458 (25.93%)	2,398,607 (25.96%)	813,562 (8.81%)	691,296 (7.48%)	2,939,779 (31.82%)
2071–2100, RCP4.5–SSP2	9,060,455	1,290,137 (14.24%)	2,590,904 (28.60%)	1,012,872 (11.18%)	748,978 (8.27%)	3,417,564 (37.72%)

2071–2100, RCP8.5–SSP5	10,609,571	977,148 (9.21%)	2,501,657 (23.58%)	1,221,078 (11.51%)	887,637 (8.37%)	5,022,051 (47.34%)

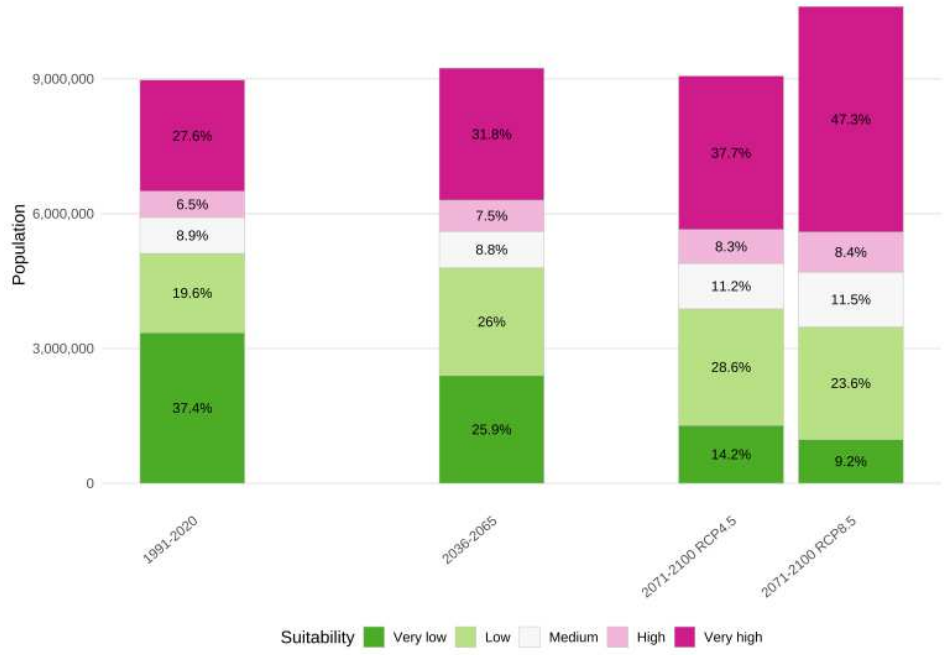


Figure 9. Population by habitat-suitability class for the reference period and three future climate–population scenarios. Percent labels refer to the share of the population represented in each scenario.

4. Discussion

Current and future habitat in Austria

This study reveals that current high suitability is highly localised in populated urban and peri-urban lowlands, while most alpine regions remain below the observation-derived thresholds. All future scenarios shift the national HSI distribution towards higher suitability, with the greatest expansion under late-century RCP8.5. Additional major findings include that high and very-high classes remain much more spatially restricted than the broader medium class, indicating that expanding climatic feasibility does not translate uniformly into core habitat. Climate-model uncertainty is greatest in transition zones rather

than in consistently suitable urban cores or consistently unsuitable high mountains. Another major finding is that the broad spatial pattern is stable under moderate local perturbations of the expert weights, although continuous values and class assignment are more sensitive near environmental and classification boundaries.

These findings support the assumption that present suitability is concentrated in low-elevation urban environments with mild winters and that warming will facilitate expansion along eastern lowlands and major valley systems. The integration of land-cover is central because urban association can arise from several mechanisms: artificial container availability, warmer microclimates, human host density, introduction pressure and reporting effort. The model represents the first two indirectly through imperviousness, settlement classes, fragmentation and woody vegetation, but does not explicitly model hosts, mobility or observation effort. Urban catch basins and other sheltered sites can be warmer and less thermally variable than gridded winter climate, increasing local overwintering potential and demonstrating why macroclimate alone may underestimate establishment risk (Ravasi et al., 2018, 2022).

The population analysis demonstrates that relatively limited spatial expansion can disproportionately affect a substantial number of residents because suitability coincides with higher populated settlement areas. Agreement with known populations supports ecological plausibility but does not constitute independent validation, because the presence records also define the class thresholds. The results show that expected future warming does not uniformly convert Austria into suitable habitat. High HSI occurs where suitable climate and environmental habitat coincide, and urban or peri-urban settings remain the principal cores since climatic constraints will remain in future. Woody vegetation and fragmented settlement mosaics may provide shade and resting habitat, but densely forested environments may

contain fewer artificial containers and human hosts. Their net suitability remains uncertain and should be tested through stratified monitoring rather than assumed from individual land-cover indicators.

Citizen science data and data-driven modelling

The projected increase in habitat suitability is consistent with European assessments identifying winter cold and insufficient summer warmth as important constraints on *Ae. albopictus* establishment and anticipating northward and altitudinal expansion under climate change (Caminade et al., 2012; Fischer et al., 2011, 2014; Kraemer et al., 2019; Oliveira et al., 2021). The Austrian patterns also accord with evidence that the species can expand rapidly into climatically favourable environments where introduction pressure and suitable local habitat permit establishment (Radici et al., 2025). Direct numerical comparison among studies remains difficult because model resolution, climate periods and response variables differ, and because predicted quantities may represent climatic suitability, current occurrence, establishment probability or seasonal population dynamics.

Compared with continental climate-focused assessments, the present model produces a more spatially restricted pattern of high suitability because climatic feasibility is moderated by nationally resolved settlement and land-cover conditions. This difference reflects model purpose rather than conflicting ecological conclusions. Broad-scale studies primarily delineate the potential climatic niche, whereas the present index identifies where favourable summer climate, overwintering conditions and settlement-associated habitat overlap at 1 km resolution in a topographically complex country. It is therefore intended principally as a transparent surveillance-prioritisation framework rather than as a direct statistical estimate of occurrence probability.

The approach is complementary to correlative, machine-learning and mechanistic models. Data-driven species distribution models can capture nonlinear relationships and interactions that are difficult to specify through expert rules, while process-based models such as *dynamAedes* explicitly represent

551 temperature-dependent development and seasonal population dynamics (Da Re et al., 2022). Recent
552 studies demonstrate the potential of citizen-science observations for invasive-mosquito modelling when
553 these data are supported by sufficiently large samples and independent surveillance. In Hungary, citizen-
554 science-informed distribution models were evaluated against direct trapping, with successful
555 independent validation for *Ae. albopictus* but not consistently for the other invasive Aedes species
556 considered (Garamszegi et al., 2025). In Spain, citizen science has provided detections that complement
557 the precision of conventional field surveillance by offering broader and more rapid spatial coverage
558 (Eritja et al., 2025). Combining Mosquito Alert observations with trap data has also been shown to
559 broaden the environmental conditions represented in the training data and improve temporal predictive
560 performance (Cerecedo-Iglesias et al., 2026).

561 A growing methodological literature addresses the biases inherent in opportunistic presence-only data.
562 Target-group background sampling can reduce bias where the focal species and the selected background
563 taxa share a comparable observation process, although performance depends on how closely the target
564 group reproduces the focal species' sampling bias (Botella et al., 2020; Phillips et al., 2009). Multi-species
565 models can go further by jointly estimating spatial sampling effort and habitat suitability from
566 opportunistic records (Botella et al., 2021), while observer-specific information, accessibility covariates
567 and refined background-selection procedures can be used to represent additional components of the
568 observation process (Chauvier et al., 2021). Lasgorceux et al. (2026) provide one recent example in which
569 aggregated reports of a broader taxonomic group were used as a proxy for spatio-temporal sampling
570 effort within a hierarchical presence-only model. Such approaches show considerable promise, but their
571 assumptions and performance depend strongly on the structure and volume of the available data.

572 Direct application of these methods to the current Austrian mosquito dataset would be challenging. The
573 available time series is shorter and contains substantially fewer observations than many applications

developed from mature citizen-science databases. Reporting intensity is also unlikely to be homogeneous among mosquito taxa. *Ae. albopictus* is conspicuous, receives considerable public and media attention, and may be submitted with a different probability from native mosquitoes or less readily identifiable invasive species. Repeated records from known urban populations, local awareness campaigns and spatial variation in app participation may therefore create a reporting process that cannot be represented reliably by simply pooling all mosquito observations as a target group. Mosquito Alert analyses in Barcelona have demonstrated that reporting effort can vary with population density and neighbourhood characteristics and that correcting for this spatial structure can materially affect predicted mosquito distributions (Padilla-Pozo et al., 2024). A recent master's thesis tested a data-driven spatio-temporal modelling approach for Graz with promising results (Knabe, 2025). The study assumed broadly homogeneous sampling effort and compared approaches for controlling sampling bias.

A further context-specific complication is that *Ae. albopictus* is still colonising Austria. A location without a record may be environmentally unsuitable, insufficiently sampled, not yet reached by the species, or subject to low and intermittent introduction pressure. Consequently, pseudo-absences or background points generated from currently unoccupied areas could cause a statistical model to interpret invasion history as an environmental limitation. The species' realised distribution is therefore not yet in equilibrium with the full range of potentially suitable habitats. For expanding invasive species, iterative updating as new regions are colonised may be more informative than treating a single early-stage distribution as a complete representation of the environmental niche (Santana et al., 2024).

More advanced data-driven modelling nevertheless represents an important future development. App-derived measures of participant activity, total mosquito submissions, accessibility, population density and public-awareness campaigns could be evaluated as proxies for the observation process. These could be combined with repeated Ovitrap detections and non-detections in integrated or hierarchical models,

thereby exploiting the broad coverage of citizen science while anchoring inference with structured surveillance. Models should be evaluated using spatial and temporal cross-validation and, wherever possible, independent trap data, because performance measured against the same biased observations used for calibration may provide an overly favourable assessment (Baker et al., 2024).

At the present stage of colonisation, the expert-informed index provides a transparent means of mapping environmental potential without fitting ecological responses directly to a spatially incomplete invasion pattern. As the surveillance network, temporal record and geographic coverage expand, the index can serve as a benchmark against which presence-background, integrated citizen-science, dynamic occupancy and mechanistic population models are compared. Such model comparison would help determine when the Austrian observation base has become sufficiently representative to support a transition from expert-informed habitat suitability towards empirically estimated occurrence and colonisation dynamics.

Austria also has Ovitrap monitoring data, providing repeated observations of egg occurrence and abundance at monitored sites. Because Ovitraps measure oviposition rather than the predominantly adult mosquitoes reported through Mosquito Alert, they offer complementary evidence of local reproductive activity and potential establishment (Bakran-Lebl et al., 2026). They also constitute an important independent monitoring resource for future evaluation and data-driven modelling. However, trap locations are spatially targeted rather than representative of Austria as a whole and are concentrated mainly in urban areas and locations already considered favourable or at elevated invasion risk (Supplementary Figure 4). Positive detections and zero counts are therefore conditional on the monitoring design, limiting their interpretation as unbiased presence–absence data.

The suitability and uncertainty maps resulting from this study could support a more stratified extension of the existing monitoring network. Additional sites could be selected across combinations of high and

low suitability, high and low uncertainty, projected range margins, and comparable urban and non-urban environments. Sampling in predicted medium- to high-suitability or uncertain cells, including variation in land-use and -cover such as semi-natural settings, would provide more informative non-detection data and help distinguish ecological limitation from under-sampling. This would complement citizen-science observations, which offer broad spatial coverage and expert-validated detections but remain influenced by population density, accessibility and public engagement and cannot provide systematic absence information free of bias (Južnič-Zonta et al., 2022).

Interpretation of uncertainty

Three distinct sources of uncertainty are represented in this study. Climate-projection uncertainty is expressed by the spread among the 16 ÖKS15 ensemble members, whereas weighting uncertainty reflects variation in the HSI resulting from Monte Carlo perturbation of the expert-derived domain and indicator weights. Classification uncertainty arises when changes in the continuous HSI, or in the thresholds used to translate it into classes, cause cells to move between suitability categories. These components address different questions and should not be interpreted interchangeably. Moreover, neither analysis captures the full range of uncertainty associated with alternative emissions pathways, future land-cover change, species adaptation, introduction pressure, observation bias or the structural assumptions of the index model.

The bivariate maps place projected mean suitability in the context of climate-model agreement. Areas combining high mean suitability with low ensemble spread represent comparatively consistent projected hotspots, whereas areas with moderate or high suitability and greater ensemble spread identify transition zones where the projected outcome depends more strongly on the climate realisation. Conversely, low ensemble spread in alpine areas indicates agreement among the climate models on low modelled suitability; it does not establish ecological absence or exclude transient introductions or locally

favourable microhabitats. Regions with high mean suitability and low uncertainty provide the strongest basis for prioritising surveillance, while areas with medium or high mean suitability and high uncertainty should be considered for adaptive monitoring and periodic reassessment.

The close correspondence between the reference HSI and the Monte Carlo ensemble of the sensitivity analysis together with the high reference-class agreement reported in the supplementary sensitivity analysis, indicates that the principal suitability pattern is not dependent on one exact weighting configuration (see Supplementary Material).

Population exposure and public-health implications

Population exposure provides a public-health interpretation of habitat suitability by identifying where environmentally receptive areas coincide with resident human populations. In this study, exposure refers to the number of people living in areas where environmental conditions may support *Ae. albopictus* establishment, and therefore indicates potential exposure to the vector itself, including nuisance biting and the need for surveillance or control. It does not represent disease incidence, mosquito abundance or human infection risk.

Transmission of arboviruses such as dengue or chikungunya viruses would require additional conditions beyond habitat suitability. Local transmission of arboviruses such as dengue and chikungunya viruses becomes possible only when competent and seasonally active mosquito populations, favourable thermal conditions for virus replication, susceptible human populations and the introduction of an infectious arbovirus coincide (Medlock et al., 2012; Rezza et al., 2007; Mordecai et al., 2019). Such introductions may originate from endemic regions or from areas experiencing active transmission in southern Europe during the summer travel season. Previous European outbreaks illustrate this pathway, including the 2007 chikungunya outbreak in Emilia-Romagna, which followed an imported infection and resulted in

665 more than 200 locally acquired cases, and the 2024 dengue outbreak in Fano, Italy, where 199
666 autochthonous cases were reported (Rezza et al., 2007; Sacco et al., 2024).

667 The exposure analysis therefore adds a demographic dimension to environmental suitability but should
668 not be interpreted as a prediction of outbreak probability or case numbers, but as population exposed
669 and potentially affected by *Ae. albopictus*. Because Austria's population is concentrated in lowland
670 settlements and urban transport corridors, even a modest expansion of suitable habitat may encompass
671 a comparatively large number of residents. Both absolute counts and population shares are relevant, as
672 the SSP scenarios differ marginally in total population and spatial distribution. Differences between
673 historical and future exposure also reflect the combined effects of changing suitability and the
674 assumptions embedded in the respective population datasets.

675 The estimates describe population residing within modelled suitable habitat, not disease burden or
676 transmission probability. They do not include mosquito abundance, duration of seasonal activity, biting
677 rates, pathogen importation, temperature-dependent extrinsic incubation, human behaviour or vector-
678 control capacity. Actual transmission risk depends on additional processes not represented in the
679 exposure metric, including pathogen introduction, seasonal mosquito abundance, temperature-
680 dependent pathogen development and vector competence, human–vector contact, case detection and
681 the timing and effectiveness of control measures. A more complete assessment would therefore
682 integrate the habitat and exposure layers with travel-related importation pressure, human mobility and
683 dynamic vector and transmission models. Such integration would provide a basis for estimating within-
684 season transmission potential rather than environmental receptivity alone.

685 The combined suitability, uncertainty and exposure results support a risk-informed surveillance strategy.
686 Areas with high suitability and low uncertainty are priorities for sustained Ovitrap monitoring, public
687 communication and rapid-response capacity, whereas high-uncertainty transition zones are particularly

688 valuable for exploratory monitoring and model updating. Transport-connected locations should remain
689 priorities even where local suitability is moderate because repeated introductions may precede
690 establishment. Surveillance should also include stratified sampling across suitability and uncertainty
691 classes rather than being restricted to predicted hotspots. This would provide more informative non-
692 detections and reduce the circularity that arises when observations from known urban populations are
693 used to interpret a model that already includes urban predictors. Mosquito Alert remains valuable for
694 early detection and broad public coverage, but its expert-validated presence records cannot substitute
695 for probability-based monitoring or reliable absence information (Južnič-Zonta et al., 2022). From a
696 climate-adaptation perspective, the maps indicate where surveillance and response capacity may need
697 to expand before establishment and local transmission become more widespread.

698 **Limitations and future research**

699 Several limitations should be considered when interpreting the model outputs. First, the habitat
700 suitability index represents relative environmental suitability rather than occurrence probability,
701 mosquito abundance, colonisation timing or disease risk. Environmentally suitable cells may remain
702 unoccupied in the absence of introduction, whereas repeated transport can generate transient
703 detections in locations that do not support persistent populations. The maps should therefore be
704 interpreted as estimates of environmental receptivity conditional on arrival, rather than predictions of
705 where *Ae. albopictus* will necessarily occur.

706 Second, the weighted arithmetic aggregation is linear and compensatory: low suitability for one indicator
707 can be offset by favourable values for others. This may overestimate overall suitability where a single
708 ecological process, such as exposure to lethal winter temperatures, acts as a strict limiting factor. The
709 selected ecological thresholds, indicator transformations and the inversion of heavy-precipitation
710 frequency are also structural assumptions that require further empirical evaluation. Alternative

711 formulations using non-linear response functions, limiting-factor rules or partially non-compensatory
712 aggregation could therefore be compared with the present model.

713 The citizen-science observations used to derive the suitability classes introduce a further source of
714 uncertainty. Reports are concentrated in populated, accessible and highly engaged areas, and reporting
715 intensity is influenced by public awareness, known infestations and observer activity. Repeated records
716 from established populations were not spatially thinned. This allows cells with frequent verified
717 detections to exert greater influence on the observation-derived thresholds, which may be ecologically
718 defensible because repeated presence can indicate sustained local suitability or establishment rather
719 than an isolated introduction. However, the same pattern can also arise from repeated sampling and
720 heightened reporting effort in known hotspots. The resulting classification therefore reflects a
721 combination of environmental suitability, establishment history and observation intensity. Because the
722 data contain verified presences but no systematic absences, they cannot provide an unbiased national
723 validation of the model. However, a qualitative evaluation was undertaken using Ovitrap data
724 (Supplementary Figure 4). Although independent of the citizen-science records, these data are also
725 subject to spatial targeting bias.

726 The spatial resolution and treatment of environmental change impose additional constraints. Land cover
727 was held constant across future scenarios, excluding urban expansion, vegetation change, altered water-
728 management practices and behavioural responses such as increased domestic water storage. The 1 km
729 grid captures regional climatic and land-cover gradients but cannot resolve microhabitats such as
730 gardens, artificial containers, courtyards, drainage systems or other fine-scale habitats. Urban
731 microclimates may also differ substantially from gridded or station-based climate data; for example,
732 sheltered stormwater infrastructure can provide warmer and more thermally stable overwintering
733 conditions than the surrounding environment (Ravasi et al., 2018, 2022).

Uncertainty estimates remain conditional on the assumptions and datasets evaluated. The Monte Carlo analysis demonstrated that the broad spatial pattern was stable under progressively wider perturbations of the expert-derived weights, but it retained the same indicators, transformations, hierarchical structure and additive aggregation rule. It therefore does not constitute a global assessment of all plausible model structures. Similarly, ensemble standard deviation represents variation among the selected ÖKS15 climate members and does not encompass the full uncertainty associated with emissions pathways, downscaling methods, ecological adaptation or future land-cover change. Historical and future exposure estimates also rely on different population products and scenario assumptions, so changes in exposure reflect both projected suitability and demographic change. Model outcomes consequently remain conditional on the selection, transformation and weighting of indicators. Although these choices are ecologically plausible and grounded in the literature and expert knowledge, they directly influence the representation of habitat suitability and all analyses derived from it.

The model does not explicitly represent introduction pressure or dispersal. Road traffic, freight transport, tourism, human mobility, distance from established populations and repeated introductions are likely to influence the sequence and timing of colonisation. Other omitted factors include relative humidity, container density, vector-control intensity and possible evolutionary or behavioural adaptation. The habitat maps are therefore best interpreted as a basis for surveillance prioritisation rather than as forecasts of short- to long-term invasion dynamics.

Future work should prioritise independent evaluation and systematic data collection to support data-driven modelling approaches. A stratified Ovitrap network spanning combinations of suitability and uncertainty would provide repeated detections, non-detections and egg-count data under a more systematic sampling design. Monitoring should ideally include not only established hotspots, but also uncertain transition zones and locations classified as having low suitability, including selected non-urban

and semi-natural environments. Such data would allow the model's discrimination, calibration and temporal transferability to be assessed, while also clarifying whether repeated citizen-science records reflect ecological suitability, observation effort or both.

The current Ovitrap network already provides a valuable complementary dataset because it measures oviposition activity rather than predominantly adult mosquito reports. However, trap locations are themselves targeted towards urban areas and locations of known or suspected risk. Future expansion towards a more stratified design would improve the representation of the environmental gradient and provide more informative non-detections. These observations could then be used to train data-driven models and benchmark the expert-informed index against correlative, integrated citizen-science and mechanistic models.

Finally, coupling environmental suitability with seasonal mosquito abundance, pathogen importation, temperature-dependent viral development and human mobility would permit progression from habitat exposure towards epidemiological risk assessment. Such extensions would help distinguish areas that are environmentally suitable from those where the seasonal coincidence of vectors, imported infections and human populations creates a meaningful risk of local transmission.

5. Conclusion

This study provides a nationally consistent assessment of current and future environmental suitability for *Ae. albopictus* in Austria. Under present conditions, suitable habitat is concentrated mainly in urban lowlands and major valley systems, while extensive alpine areas remain thermally constrained. All future scenarios indicate an expansion and intensification of suitability, with the strongest changes projected for 2071–2100 under RCP8.5. The proportion of Austria classified as Very low suitability declines from 92.3% in the reference period to 59.1% under late-century RCP8.5, while Medium to Very high suitability

779 expands from 1.6% to 6.1%. Although the highest suitability classes remain spatially concentrated, their
780 overlap with densely populated lowland and urban areas results in a substantial increase in population
781 exposure. Under late-century RCP8.5, the number of residents in cells classified as High or Very high
782 suitability increases from approximately 3.06 million under reference conditions to 5.91 million, driven
783 mainly by an increase in the Very high class from 2.48 million to 5.02 million residents.

784 The climate ensemble and Monte Carlo analyses show that uncertainty is spatially structured rather than
785 uniform. Climate-model disagreement is greatest in transition zones, particularly parts of the Alpine
786 foreland, whereas several urban hotspots show high suitability with greater uncertainty at mid-century
787 but stronger ensemble agreement under late-century RCP8.5 as the warming signal becomes more
788 pronounced. The broad suitability pattern was also robust to the expert-derived weighting assumptions.
789 Even under the broadest Dirichlet perturbation scenario, the modal class differed from the reference
790 over only 0.65% of the modelled area when observation-derived thresholds were recalculated and 2.07%
791 when the original thresholds were held fixed. Nevertheless, wider uncertainty intervals and more
792 frequent threshold crossing in lowland and urban areas demonstrate that local interpretations should
793 rely on the spatial uncertainty maps rather than national agreement statistics alone.

794 The hierarchical index offers a transparent and reproducible framework for an early stage of invasion,
795 when occurrence records remain clustered, opportunistic and strongly influenced by introduction history
796 and reporting effort. By integrating climate, land cover, observation-anchored classification, population
797 exposure and explicit uncertainty analysis, the model provides a practical basis for prioritising
798 surveillance and climate-adaptation planning. Its outputs represent relative environmental suitability
799 and receptivity, not occurrence probability, colonisation timing or disease risk. Local transmission
800 additionally depends on vector abundance, pathogen importation, human mobility, seasonal
801 transmission conditions and control effectiveness.

Future development should combine the present framework with systematic Ovitrap monitoring, improved representation of urban microhabitats and introduction pressure, and data-driven or mechanistic models as the Austrian observation base expands. Stratified monitoring across suitability and uncertainty classes, including predicted low-suitability and currently under-sampled environments, would provide the independent detections and non-detections needed to test model transferability. The present model should therefore be viewed as an iterative surveillance-prioritisation framework whose ecological assumptions and spatial predictions can be progressively evaluated and updated as colonisation and monitoring continue.

Declarations

Ethics approval and consent to participate

Not applicable. This study used existing environmental, climatic, population and mosquito observation datasets and did not involve experiments on humans or animals or the collection of identifiable personal information.

Consent for publication

Not applicable.

Availability of data and materials

The classified habitat suitability rasters generated during this study will be made available to the public following publication at data.hub.geosphere.at. The underlying climate, land-cover, population and mosquito observation datasets were obtained from SPARTACUS, ÖKS15, the Copernicus Land Monitoring Service, Statistik Austria, Pop-AUT and Mosquito Alert,

822 respectively, and are subject to the access and licensing conditions of their respective data
823 providers.

824 **Code availability**

825 R scripts used for indicator calculation, habitat suitability modelling, classification, ensemble
826 uncertainty analysis and sensitivity analysis are available from the corresponding author upon
827 reasonable request.

828 **Funding**

829 This research was funded by the Austrian Research Promotion Agency (FFG) through the KIRAS
830 programme as part of the ClimateDiseaseRisk project.

831 **Authors' contributions**

832 R.S. conceptualised the modelling framework, implemented the spatial analyses and drafted the
833 manuscript. J.W. contributed to climate-data processing and model implementation. B.S.
834 undertook a literature review and contributed to interpretation. S.K. contributed to funding
835 acquisition, conceptualisation of the study and manuscript revision. K.B.-L. contributed
836 entomological expertise, monitoring data interpretation and manuscript revision. All authors
837 reviewed and approved the manuscript.

838 **Competing interests**

839 The authors declare that they have no competing interests.

References

Arulmukavarathan A, Gilio LS, Hedrich N, Nicholas N, Reuland NI, Sheikh AR, et al. Dengue in France in 2024 - A year of record numbers of imported and autochthonous cases. New Microbes New Infect. 2024;62:101553.

Baker, D.J., Maclean, I.M.D. and Gaston, K.J., 2024. Effective strategies for correcting spatial sampling bias in species distribution models without independent test data. Diversity and Distributions 30: e13802. https://doi.org/10.1111/ddi.13802.

Bakran-Lebl, K. and Reichl, J., 2023. Ovitrap-Monitoring gebietsfremder Gelsenarten in Österreich – Jahresbericht 2022. AGES – Österreichische Agentur für Gesundheit und Ernährungssicherheit GmbH, Vienna, Austria.

Bakran-Lebl, K., Zittra, C., Harl, J., Shahi-Barogh, B., Grätzl, A., Ebmer, D., Schaffner, F. and Fuehrer, H.-P., 2021. Arrival of the Asian tiger mosquito, Aedes albopictus (Skuse, 1895), in Vienna, Austria and initial monitoring activities. Transboundary and Emerging Diseases 68: 3145–3150. *https://doi.org/10.1111/tbed.14169*.

Bakran-Lebl, K., Kopacka, I., Seebacher, B. *et al.* Tracking the Asian tiger mosquito (*Aedes albopictus*) in Austria: benefits of combining expert-based monitoring with citizen science data. *Parasites Vectors* 19, 390 (2026). https://doi.org/10.1186/s13071-026-07574-z

Benedum, C.M., Seidahmed, O.M.E., Eltahir, E.A.B. and Markuzon, N., 2018. Statistical modeling of the effect of rainfall flushing on dengue transmission in Singapore. PLOS Neglected Tropical Diseases 12: e0006935. https://doi.org/10.1371/journal.pntd.0006935.

Botella, C., Joly, A., Monestiez, P., Bonnet, P. and Munoz, F., 2020. Bias in presence-only niche models related to sampling effort and species niches: lessons for background point selection. PLOS ONE 15: e0232078. https://doi.org/10.1371/journal.pone.0232078.

Botella, C., Joly, A., Bonnet, P., Munoz, F. and Monestiez, P., 2021. Jointly estimating spatial sampling effort and habitat suitability for multiple species from opportunistic presence-only data. Methods in Ecology and Evolution 12: 933–945. https://doi.org/10.1111/2041-210X.13565.

Bouzid, M., Colón-González, F.J., Lung, T., Lake, I.R. and Hunter, P.R., 2014. Climate change and the emergence of vector-borne diseases in Europe: case study of dengue fever. BMC Public Health 14: 781. https://doi.org/10.1186/1471-2458-14-781.

Caminade, C., Medlock, J.M., Ducheyne, E., McIntyre, K.M., Leach, S., Baylis, M. and Morse, A.P., 2012. Suitability of European climate for the Asian tiger mosquito Aedes albopictus: recent trends and future scenarios. Journal of the Royal Society Interface 9: 2708–2717. https://doi.org/10.1098/rsif.2012.0138.

Cariboni, J., Gatelli, D., Liska, R. and Saltelli, A., 2007. The role of sensitivity analysis in ecological modelling. Ecological Modelling 203: 167–182. https://doi.org/10.1016/j.ecolmodel.2005.10.045.

Cerecedo-Iglesias, C., Palmer, J.R.B. and Bartumeus, F., 2026. Citizen science deepens the ecological and climatic dimensions of mosquito surveillance. Ecography: e08414. https://doi.org/10.1002/ecog.08414.

Chauvier, Y., Zimmermann, N.E., Poggiato, G., Bystrova, D., Brun, P. and Thuiller, W., 2021. Novel methods to correct for observer and sampling bias in presence-only species distribution models. Global Ecology and Biogeography 30: 2312–2325. https://doi.org/10.1111/geb.13383.

Chimani, B., Heinrich, G., Hofstätter, M., Kerschbaumer, M., Kienberger, S., Leuprecht, A., Lexer, A., Peßenteiner, S., Poetsch, M.S., Salzmann, M., Spiekermann, R., Switanek, M. and Truhetz, H., 2016. ÖKS15 – Klimaszenarien für Österreich: Daten, Methoden und Klimaanalyse. Project final report, Vienna, Austria.

Da Re, D., Van Bortel, W., Reuss, F., Müller, R., Boyer, S., Montarsi, F., Ciocchetta, S., Arnoldi, D., Marini, G., Rizzoli, A., L'Ambert, G., Lacour, G., Koenraadt, C.J.M., Vanwambeke, S.O. and Marcantonio, M., 2022. dynamAedes: a unified modelling framework for invasive Aedes mosquitoes. Parasites & Vectors 15: 414. https://doi.org/10.1186/s13071-022-05414-4.

Eritja, R., Sanpera-Calbet, I., Delacour-Estrella, S., Ruiz-Arrondo, I., Puig, M.À., Bengoa-Paulís, M., Alarcón-Elbal, P.M., Barceló, C., Mariani, S., Martínez-Barciela, Y., Bravo-Barriga, D., Polina, A., Pereira-Martínez, J.M., González, M.A., Escartin, S., Melero-Alcíbar, R., Blanco-Sierra, L., Magallanes, S., Collantes, F., Ferraguti, M., González-Pérez, M.I., Gutiérrez-López, R., Silva-Torres, M.I., San Sebastián-Mendoza, O., Calvo-Reyes, M.C., Mendoza-García, M., Macías-Magro, D., Cisneros, P., Cevidanes, A., Frontera, E., Mato, I., Fúster-Lorán, F., Domench-Guembe, M., Rodríguez-Regadera, M.E., Casanovas-Urgell, R., Montalvo, T., Miranda, M.Á., Figuerola, J., Lucientes-Curdi, J., Garriga, J., Palmer, J.R.B. and Bartumeus, F., 2025. Integrating citizen science and field sampling into next-generation early-warning systems for vector surveillance: twenty years of municipal detections of Aedes invasive mosquito species in Spain. Insects 16: 904. https://doi.org/10.3390/insects16090904.

European Centre for Disease Prevention and Control (ECDC), 2025a. Historical data on local transmission of dengue in the EU/EEA. Available at: https://www.ecdc.europa.eu/en/all-topics-z/dengue/surveillance-and-disease-data/autochthonous-transmission-dengue-virus-eueea-previous-years.

903 European Centre for Disease Prevention and Control (ECDC), 2025b. Public health guidance for assessing
904 and mitigating the risk of locally acquired Aedes-borne viral diseases in the EU/EEA. ECDC,
905 Stockholm, Sweden. Available at:
906 https://www.ecdc.europa.eu/sites/default/files/documents/guidance-for-assessing-risk-locally-
907 acquired-Aedes.pdf.

908 European Centre for Disease Prevention and Control (ECDC) and European Food Safety Authority (EFSA),
909 2025. Mosquito maps. Available at: https://www.ecdc.europa.eu/en/disease-vectors/surveillance-
910 and-disease-data/mosquito-maps.

911 Evans, M.V., Hintz, C.W., Jones, L., Shiau, J.C., Solano, N., Drake, J.M. and Murdock, C.C., 2019.
912 Microclimate and larval habitat density predict adult Aedes albopictus abundance in urban areas.
913 American Journal of Tropical Medicine and Hygiene 101: 362–370.
914 https://doi.org/10.4269/ajtmh.19-0220.

915 Fischer, D., Thomas, S.M., Niemitz, F., Reineking, B. and Beierkuhnlein, C., 2011. Projection of climatic
916 suitability for Aedes albopictus Skuse (Culicidae) in Europe under climate change conditions. Global
917 and Planetary Change 78: 54–64. https://doi.org/10.1016/j.gloplacha.2011.05.008.

918 Fischer, D., Thomas, S.M., Neteler, M., Tjaden, N.B. and Beierkuhnlein, C., 2014. Climatic suitability of
919 Aedes albopictus in Europe referring to climate change projections: comparison of mechanistic and
920 correlative niche modelling approaches. Eurosurveillance 19: 20696. https://doi.org/10.2807/1560-
921 7917.ES2014.19.6.20696.

922 Formayer, H., Parajka, J. and Petermann, J.S., 2025. Chapter 1. Physical and ecological manifestation of
923 climate change in Austria. Verlag der Österreichischen Akademie der Wissenschaften, Vienna,
924 Austria. *https://doi.org/10.1553/aar2-ch1*.

Fournier L, Durand GA, Cochet A, Brottet E, Fiet C, Mano Q, et al. Multiple early local transmissions of chikungunya virus, Mainland France, from May 2025. Eurosurveillance. 2025;30:2500545. *https://doi.org/10.2807/1560-7917.ES.2025.30.32.2500545*

Garamszegi, L.Z., Soltész, Z., Szentiványi, T., Kurucz, K., Nagy, G. and Bede-Fazekas, Á., 2025. Identifying ecological factors mediating the spread of three invasive mosquito species: citizen science informed prediction. Journal of Pest Science 98: 913–928. https://doi.org/10.1007/s10340-024-01841-7.

Hiebl, J. and Frei, C., 2016. Daily temperature grids for Austria since 1961—concept, creation and applicability. Theoretical and Applied Climatology 124: 161–178. https://doi.org/10.1007/s00704-015-1411-4.

Hiebl, J. and Frei, C., 2018. Daily precipitation grids for Austria since 1961—development and evaluation of a spatial dataset for hydroclimatic monitoring and modelling. Theoretical and Applied Climatology 132: 327–345. *https://doi.org/10.1007/s00704-017-2093-x*.

IPCC. 2014. Climate Change 2014: Synthesis Report. Contribution of Working Groups I, II and III to the Fifth Assessment Report of the Intergovernmental Panel on Climate Change. Edited by R.K. Pachauri and L.A. Meyer. Geneva, Switzerland: IPCC.

Johnson, C.J. and Gillingham, M.P., 2004. Mapping uncertainty: sensitivity of wildlife habitat ratings to expert opinion. Journal of Applied Ecology 41: 1032–1041. https://doi.org/10.1111/j.0021-8901.2004.00975.x.

Južnič-Zonta, Ž., Sanpera-Calbet, I., Eritja, R., Palmer, J.R.B., Escobar, A., Garriga, J., Oltra, A., Richter-Boix, A., Schaffner, F., Della Torre, A., Miranda, M.Á., Koopmans, M.P.G., Barzon, L., Bartumeus, F., Mosquito Alert Digital Entomology Network and Mosquito Alert Community, 2022. Mosquito Alert:

leveraging citizen science to create a GBIF mosquito occurrence dataset. GigaByte 2022: 54. https://doi.org/10.46471/gigabyte.54.

Knabe, D., 2025. Predicting the spatio-temporal presence of Aedes albopictus in Graz, Austria, using citizen science network data. Master's thesis, University of Vienna, Vienna, Austria.

Koenraadt, C.J.M. and Harrington, L.C., 2008. Flushing effect of rain on container-inhabiting mosquitoes Aedes aegypti and Culex pipiens (Diptera: Culicidae). Journal of Medical Entomology 45: 28–35.

Kraemer, M.U.G., Reiner, R.C. Jr, Brady, O.J., Messina, J.P., Gilbert, M., Pigott, D.M., Yi, D., Johnson, K., Earl, L., Marczak, L.B., Shirude, S., Weaver, N.D., Bisanzio, D., Perkins, T.A., Lai, S., Lu, X., Jones, P., Coelho, G.E., Carvalho, R.G., Van Bortel, W., Marsboom, C., Hendrickx, G., Schaffner, F., Moore, C.G., Nax, H.H., Bengtsson, L., Wetter, E., Tatem, A.J., Brownstein, J.S., Smith, D.L., Lambrechts, L., Cauchemez, S., Linard, C., Faria, N.R., Pybus, O.G., Scott, T.W., Liu, Q., Yu, H., Wint, G.R.W., Hay, S.I. and Golding, N., 2019. Past and future spread of the arbovirus vectors Aedes aegypti and Aedes albopictus. Nature Microbiology 4: 854–863. https://doi.org/10.1038/s41564-019-0376-y.

Lasgorceux, F., Papaïx, J., Bunz, Y., Combrisson, D. and Opitz, T., 2026. Space-time species distribution modeling with opportunistic presence-only data: a case study of passerines in a protected area. Peer Community Journal 6: e52. https://doi.org/10.24072/pcjournal.731.

Li, Y., Kamara, F., Zhou, G., Puthiyakunnon, S., Li, C., Liu, Y., Zhou, Y., Yao, L., Yan, G. and Chen, X.-G., 2014. Urbanization increases Aedes albopictus larval habitats and accelerates mosquito development and survivorship. PLOS Neglected Tropical Diseases 8: e3301. https://doi.org/10.1371/journal.pntd.0003301.

966 Ligmann-Zielinska, A. and Jankowski, P., 2014. Spatially-explicit integrated uncertainty and sensitivity
967 analysis of criteria weights in multicriteria land suitability evaluation. Environmental Modelling &
968 Software 57: 235–247. https://doi.org/10.1016/j.envsoft.2014.03.007.

969 Lyberger, K.P., Robinson, A.R., Couper, L., Delwel, I., Glidden, C., Qian, C., Burslem, A., Fernandez, F., Gao,
970 B., Garcia, G., Greenland, K.B., Griffin, C., Jackson, S., King, A., Manes, O., Song, A., Tran, E., Wilairat,
971 S. and Mordecai, E.A., 2025. A scoping review of mosquito vector range shifts: widespread
972 expansions and evidence gaps in climate attribution. Global Change Biology 31: e70551.
973 https://doi.org/10.1111/gcb.70551.

974 Malczewski, J., 2006. GIS-based multicriteria decision analysis: a survey of the literature. International
975 Journal of Geographical Information Science 20: 703–726.
976 https://doi.org/10.1080/13658810600661508.

977 Marbler, A., 2024. Pop-AUT: Subnational SSP Population Projections for Austria, Version 1.0 [data set].
978 Zenodo. https://doi.org/10.5281/zenodo.10477870.

979 Marino, S., Hogue, I.B., Ray, C.J. and Kirschner, D.E., 2008. A methodology for performing global
980 uncertainty and sensitivity analysis in systems biology. Journal of Theoretical Biology 254: 178–196.
981 https://doi.org/10.1016/j.jtbi.2008.04.011.

982 Medlock, J.M., Avenell, D., Barrass, I. and Leach, S., 2006. Analysis of the potential for survival and
983 seasonal activity of Aedes albopictus (Diptera: Culicidae) in the United Kingdom. Journal of Vector
984 Ecology 31: 292–304.

985 Medlock, J.M., Hansford, K.M., Schaffner, F., Versteirt, V., Hendrickx, G., Zeller, H. and Van Bortel, W.,
986 2012. A review of the invasive mosquitoes in Europe: ecology, public health risks, and control
987 options. Vector-Borne and Zoonotic Diseases 12: 435–447. https://doi.org/10.1089/vbz.2011.0814.

Mordecai, E.A., Caldwell, J.M., Grossman, M.K., Lippi, C.A., Johnson, L.R., Neira, M., Rohr, J.R., Ryan, S.J., Savage, V., Shocket, M.S., Sippy, R., Stewart Ibarra, A.M., Thomas, M.B. and Villena, O., 2019. Thermal biology of mosquito-borne disease. Ecology Letters 22: 1690–1708. https://doi.org/10.1111/ele.13335.

Nawrocki, S.J. and Hawley, W.A., 1987. Estimation of the northern limits of distribution of Aedes albopictus in North America. Journal of the American Mosquito Control Association 3: 314–317.

Oliveira, S., Rocha, J., Sousa, C.A. and Capinha, C., 2021. Wide and increasing suitability for Aedes albopictus in Europe is congruent across distribution models. Scientific Reports 11: 9916. https://doi.org/10.1038/s41598-021-89096-5.

Padilla-Pozo, Á., Bartumeus, F., Montalvo, T., Sanpera-Calbet, I., Valsecchi, A. and Palmer, J.R.B., 2024. Assessing and correcting neighborhood socioeconomic spatial sampling biases in citizen science mosquito data collection. Scientific Reports 14: 22462. https://doi.org/10.1038/s41598-024-73416-6.

Phillips, S.J., Dudík, M., Elith, J., Graham, C.H., Lehmann, A., Leathwick, J. and Ferrier, S., 2009. Sample selection bias and presence-only distribution models: implications for background and pseudo-absence data. Ecological Applications 19: 181–197. https://doi.org/10.1890/07-2153.1.

Pianosi, F., Beven, K., Freer, J., Hall, J.W., Rougier, J., Stephenson, D.B. and Wagener, T., 2016. Sensitivity analysis of environmental models: a systematic review with practical workflow. Environmental Modelling & Software 79: 214–232. https://doi.org/10.1016/j.envsoft.2016.02.008.

Radici, A., Hammami, P., Cannet, A., L'Ambert, G., Lacour, G., Fournet, F., Garros, C., Guis, H., Fontenille, D. and Caminade, C., 2025. Aedes albopictus is rapidly invading its climatic niche in France: wider implications for biting nuisance and arbovirus control in Western Europe. Global Change Biology 31: e70414. https://doi.org/10.1111/gcb.70414.

1010 Ravasi, D., Guidi, V., Flacio, E., Lüthy, P. and Perron, K., 2018. Investigation of temperature conditions in
1011 Swiss urban and suburban microhabitats for the overwintering suitability of diapausing Aedes
1012 albopictus eggs. Parasites & Vectors 11: 212. https://doi.org/10.1186/s13071-018-2803-y.

1013 Ravasi, D., Mangili, F., Huber, D., Cannata, M., Strigaro, D. and Flacio, E., 2022. The effects of
1014 microclimatic winter conditions in urban areas on the risk of establishment for Aedes albopictus.
1015 Scientific Reports 12: 15967. https://doi.org/10.1038/s41598-022-20436-9.

1016 Reichl, J., Prossegger, C., Eichholzer, B., Plauder, P., Unterköfler, M.S., Bakran-Lebl, K., Indra, A. and
1017 Fuehrer, H.-P., 2024. A citizen science report—Tiger mosquitoes (Aedes albopictus) in allotment
1018 gardens in Graz, Styria, Austria. Parasitology Research 123: 79. https://doi.org/10.1007/s00436-023-
1019 08106-9.

1020 Rezza, G., Nicoletti, L., Angelini, R., Romi, R., Finarelli, A.C., Panning, M., Cordioli, P., Fortuna, C., Boros,
1021 S., Magurano, F., Silvi, G., Angelini, P., Dottori, M., Ciufolini, M.G., Majori, G.C. and Cassone, A., 2007.
1022 Infection with chikungunya virus in Italy: an outbreak in a temperate region. The Lancet 370: 1840–
1023 1846. https://doi.org/10.1016/S0140-6736(07)61779-6.

1024 Rocklöv, J. and Dubrow, R., 2020. Climate change: an enduring challenge for vector-borne disease
1025 prevention and control. Nature Immunology 21: 479–483. https://doi.org/10.1038/s41590-020-
1026 0648-y.

1027 Sacco, C., Liverani, A., Venturi, G., Gavaudan, S., Riccardo, F., Salvoni, G., Fortuna, C., Marinelli, K.,
1028 Marsili, G., Pesaresi, A., Molina Grané, C., Mercuri, I., Manica, M., Caucci, S., Morelli, D.,
1029 Sebastianelli, L., Marcacci, M., Ferraro, F., Di Luca, M., Pascucci, I., Merakou, C., Duranti, A., Pati, I.,
1030 Lombardini, L., Fiacchini, D., Filipponi, G., Maraglino, F., Palamara, A.T., Poletti, P., Pezzotti, P.,
1031 Filippetti, F., Merler, S., Del Manso, M., Menzo, S. and Marche Dengue Outbreak Group, 2024.

Autochthonous dengue outbreak in Fano, Italy, 2024. Eurosurveillance 29: 2400713. https://doi.org/10.2807/1560-7917.ES.2024.29.47.2400713.

Saint-Hilary, G., Cadour, S., Robert, V. and Gasparini, M., 2017. A simple way to unify multicriteria decision analysis and stochastic multicriteria acceptability analysis using a Dirichlet distribution in benefit–risk assessment. Biometrical Journal 59: 567–578. https://doi.org/10.1002/bimj.201600113.

Saisana, M., Saltelli, A. and Tarantola, S., 2005. Uncertainty and sensitivity analysis techniques as tools for the quality assessment of composite indicators. Journal of the Royal Statistical Society: Series A 168: 307–323. https://doi.org/10.1111/j.1467-985X.2005.00350.x.

Santana, J., Sillero, N., Ribeiro, J., Capinha, C., Lopes, R.J. and Reino, L., 2024. Predicting the expansion of invasive species: how much data do we need? NeoBiota 95: 109–132. *https://doi.org/10.3897/neobiota.95.122335*.

Santilli L, Canovari B, Balducci M, Corbelli G, Maracci M, Polenta A, et al. Outbreak of autochthonous dengue in Fano, Pesaro-Urbino Province - Marche region, Italy, September 2024. Infection. 2025;53:1213–8. https://doi.org/https://doi.org/10.1007/s15010-025-02476-1

Schlögl, M., Graser, A., Spiekermann, R., Lampert, J. and Steger, S., 2025. A bivariate choropleth map for visualizing uncertainty in impact-based forecasts. Natural Hazards and Earth System Sciences 25: 1425–1437. https://doi.org/10.5194/nhess-25-1425-2025.

Seidel, B., Duh, D., Nowotny, N. and Allerberger, F., 2012. Erstnachweis der Stechmücken Aedes (Ochlerotatus) japonicus japonicus (Theobald, 1901) in Österreich und Slowenien in 2011 und für Aedes (Stegomyia) albopictus (Skuse, 1895) in Österreich 2012 (Diptera: Culicidae). Entomologische Zeitschrift 122: 223–226.

1053 Situmorang, T., Bakran-Lebl, K., Unterköfler, M.S., Püschel, U., Knobloch, L. and Fuehrer, H.-P., 2025.
1054 Monitoring of alien Asian mosquitoes in Linz, Austria. Journal of the European Mosquito Control
1055 Association 43: 97–104. https://doi.org/10.52004/2054930X-20251026.

1056 Swan, T., Russell, T.L., Staunton, K.M., Field, M.A., Ritchie, S.A. and Burkot, T.R., 2022. A literature review
1057 of dispersal pathways of Aedes albopictus across different spatial scales: implications for vector
1058 surveillance. Parasites & Vectors 15: 303. https://doi.org/10.1186/s13071-022-05413-5.

1059 Thaler, S., Formayer, H., Kubu, G., Trnka, M. and Eitzinger, J., 2021. Effects of bias-corrected regional
1060 climate projections and their spatial resolutions on crop model results under different climatic and
1061 soil conditions in Austria. Agriculture 11: 1029. https://doi.org/10.3390/agriculture11111029.

1062 Thomas, S.M., Obermayr, U., Fischer, D., Kreyling, J. and Beierkuhnlein, C., 2012. Low-temperature
1063 threshold for egg survival of a post-diapause and non-diapause European aedine strain, Aedes
1064 albopictus (Diptera: Culicidae). Parasites & Vectors 5: 100. https://doi.org/10.1186/1756-3305-5-
1065 100.

1066 Thomson, M.C. and Stanberry, L.R., 2022. Climate change and vectorborne diseases. New England
1067 Journal of Medicine 387: 1969–1978. https://doi.org/10.1056/NEJMra2200092.

1068 Unterberger, C., Brunner, L., Nabernegg, S., Steininger, K.W., Steiner, A.K., Stabentheiner, E., Monschein,
1069 S. and Truhetz, H., 2018. Spring frost risk for regional apple production under a warmer climate.
1070 PLOS ONE 13: e0200201. https://doi.org/10.1371/journal.pone.0200201.

1071 Zajac, Z., Stith, B., Bowling, A.C., Langtimm, C.A. and Swain, E.D., 2015. Evaluation of habitat suitability
1072 index models by global sensitivity and uncertainty analyses: a case study for submerged aquatic
1073 vegetation. Ecology and Evolution 5: 2503–2517. https://doi.org/10.1002/ece3.1520.

1074

Supplementary Files

This is a list of supplementary files associated with this preprint. Click to download.

- Supplementaryinformation.docx